Marine Geology 357 (2014) 182–194

Contents lists available at ScienceDirect

Marine Geology

journal homepage: www.elsevier.com/locate/margeo

Late Pliocene variations of the Mediterranean outflow

Nabil Khélifi [a,b,*,1], Michael Sarnthein [a], Martin Frank [b], Nils Andersen [c], Dieter Garbe-Schönberg [a]

[a] Institute of Geosciences, Kiel University, Germany
[b] GEOMAR Helmholtz Centre for Ocean Research Kiel, Germany
[c] Leibniz-Laboratory for Radiometric Dating & Stable Isotope Research, Kiel University, Germany

ARTICLE INFO

Article history:
Received 8 June 2013
Received in revised form 10 June 2014
Accepted 23 July 2014
Available online 8 August 2014

Keywords:
Pliocene
Onset of major Northern Hemisphere Glaciation
Mediterranean Sea
Mediterranean Outflow Water
North African aridification
Atlantic Meridional Overturning Circulation
Intermediate waters

ABSTRACT

Late Pliocene changes in the advection of Mediterranean Outflow Water (MOW) derivates were reconstructed at northeast Atlantic DSDP/ODP sites 548 and 982 and compared to records of WMDW at West Mediterranean Site 978. Neodymium isotope (ε_{Nd}) values more positive than −10.5/−11 reflect diluted MOW derivates that spread almost continuously into the northeast Atlantic from 3.7 to 2.55 Ma, reaching Rockall Plateau Site 982 from 3.63 to 2.75 Ma. From 3.4 to 3.3 Ma average MOW temperature and salinity increased by 2°–4 °C and ~1 psu both at proximal Site 548 and distal Site 982. The rise implies a rise in flow strength, coeval with a long-term rise in both west Mediterranean Sea surface salinity by almost 2 psu and average bottom water salinity (BWS) by ~1 psu, despite inherent uncertainties in BWS estimates. The changes were linked with major Mediterranean aridification and a drop in African monsoon humidity. In contrast to model expectations, the rise in MOW salt discharge after 3.4 Ma did not translate into improved ventilation of North Atlantic Deep Water, since it possibly was too small to significantly influence Atlantic Meridional Overturning Circulation. Right after ~2.95 Ma, with the onset of major Northern Hemisphere Glaciation, long-term average bottom water temperature (BWT) and BWS at Site 548 dropped abruptly by ~5 °C and ~1–2 psu, in contrast to more distal Site 982, where BWT and BWS continued to oscillate at estimates of ~2 °C and 1.5–2.5 psu higher than today until ~2.6 Ma. We relate the small-scale changes both to a reduced MOW flow and to enhanced dilution by warm waters of a strengthened North Atlantic Current temporarily replacing MOW derivates at Rockall Plateau.

1. Introduction

Derivates of Mediterranean Outflow Water (MOW) constitute a tongue of warm and highly saline, moreover, nutrient-depleted and highly oxygenated waters in the northeast Atlantic at 300–1400 m water depth (w.d.), that derive from deep and intermediate waters downwelled in the Mediterranean Sea and advected through the Strait of Gibraltar (Reid, 1979; Zenk and Armi, 1990). Because of local topography and mixing processes in the Gulf of Cadiz (Borenäs et al., 2002) MOW splits into an upper (300–800 m depth, 13.5 °C, 36.5 psu) and lower limb (1100–1400 m depth, 11 °C, 37–38 psu). Due to Coriolis forcing most of the lower limb flows north forming a boundary current of meandering mesoscale eddies along the continental slope of Iberia (Käse and Zenk, 1996). Having passed the Bay of Biscay these waters reach up to Rockall Plateau (O'Neill-Baringer and Price, 1997), where they mix with North Atlantic Current (NAC) waters (McCartney and Mauritzen, 2001). Increasing salinity anomalies at the depth level of MOW in the Rockall Trough are linked with temporary contraction of the subpolar gyre and thus suggest a direct advective, albeit temporally variable, pathway (Lozier and Stewart, 2008).

On the basis of Nd isotopes (ε_{Nd}) and paired benthic $\delta^{18}O$ and Mg/Ca records our study aims to reconstruct the development of temperatures, salinities and densities, water mass transport and reach of lower MOW derivates in the context of global changes from the warm mid-Pliocene climate to the Pleistocene onset of major Northern Hemisphere Glaciation (NHG), 3.7–2.55 Ma. The records have been obtained from sediments of Deep Sea Drilling Project (DSDP) Site 548 off Brittany (1250 m w.d.) and Ocean Drilling Program (ODP) Site 982 on Rockall Plateau (1135 m w.d.) at the northeast Atlantic continental margin (Fig. 1). Horizontal and vertical anomalies of the proxies between the two sites help us to constrain past shifts in the spreading and mixing of MOW. We surmise that vertical displacements of MOW mainly reflected changes in MOW density since the mid-Pliocene, provided that the aperture of Gibraltar had been largely constant since the end of the Messinian ~5.3 Ma (Blanc, 2002).

Changes in the initial state of MOW are monitored at ODP Site 978 in the Alboran Sea (1930 m w.d.; Fig. 1). Today, this site is bathed in Western Mediterranean Deep Water (WMDW) which contributes ~33% of the MOW flux of ~0.7 Sverdrups (Tsimplis and Bryden, 2000;

* Corresponding author at: GEOMAR Helmholtz Centre for Ocean Research Kiel, Germany. Tel.: +49 431 600 2310; fax: +49 431 600 2925.
E-mail addresses: nkhelifi@geomar.de, nabil.khelifi@springer.com (N. Khélifi).
[1] Present address: Earth Sciences and Geography Editorial, Springer, Heidelberg, Germany. Tel.: +49 6221 487 8573; fax: + 49 6221 487 68573.

http://dx.doi.org/10.1016/j.margeo.2014.07.006
0025-3227/

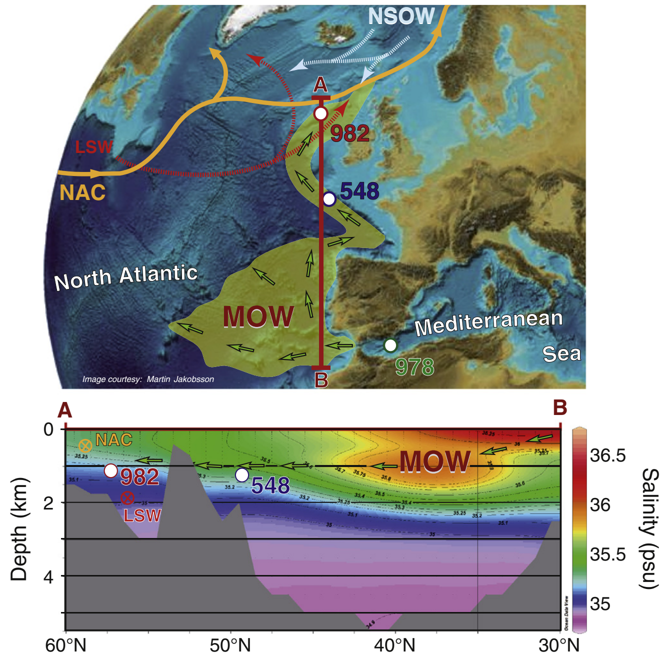

Fig. 1. Locations of Deep Sea Drilling Project (DSDP) Site 548 (48°54′N, 12°09′W, 1250 m w.d.), Ocean Drilling Program (ODP) Site 982 (57°31′N, 15°52′W, 1135 m w.d.), and ODP Site 978 (36°13′N, 2°3′W; 1930 m w.d.). (A–B) shows a modern salinity transect along the northeastern North Atlantic margin based on data of NODC (2001) and plotted using Ocean Data View (Schlitzer, 2013). NAC = North Atlantic (surface) Current. MOW = highly saline tongue of Mediterranean Sea Water (in green) centered near 1000 m w.d. (Reid, 1979). (For interpretation of the references to color in this figure legend, the reader is referred to the web version of this article.)

García-Lafuente et al., 2007). About 67% of MOW is entrained from Mediterranean Intermediate Water (Millot, 1999). In the past, the composition of these two water masses may have varied in parallel, since all Mediterranean sites of deep-water convection are controlled by largely similar climate forcings. Site 978 also has monitored long-term Pliocene changes in sea surface temperature, salinity, and climate, that finally have controlled changes of MOW density and flow strength. In the Strait of Gibraltar MOW is flowing west beneath an eastward flow of warm Atlantic surface waters (~15 °C, ~36.2 psu), a derivate of the Azores Current, which compensates for both the outflow and net evaporation loss in the Mediterranean basins (Garrett et al., 1990; Rogerson et al., 2012). When MOW cascades from the Strait of Gibraltar through the canyons of the Gulf of Cadiz, large amounts of less saline North Atlantic Central Water (NACW) are entrained from above and Labrador Sea Water (LSW) is admixed from below. Hence the volume of Mediterranean Outflow waters, hereafter called MOW derivates, is rising by a factor of 3–4 (O'Neill-Baringer and Price, 1999), whereas temperature, salinity, and density are dropping significantly (Fig. 1, lower panel).

Major changes in MOW transport are compared to deep-water paleoceanographic records obtained elsewhere in the Atlantic to investigate whether and to which degree they were linked to changes in Atlantic Meridional Overturning Circulation (AMOC), in particular, during times of long-term variations in the middle and late Pliocene (Lisiecki and Raymo, 2005; Sarnthein et al., 2009).

To enable a comprehensive understanding of long-term paleoceanographic trends we now merge our new data obtained at Site 982 (3.7–2.5 Ma) and sites 548 and 978 (3.0–2.5 Ma) with records previously published for sites 548 and 978 (3.7–3.0 Ma; Khélifi et al., 2009). This way we can (1) derive spatial trends in MOW composition, (2) monitor a MOW salinity maximum from 3.3 to 2.95 Ma at three different sites, and (3) and put the new ε_{Nd} record of Site 982 into a proper perspective with records previously measured and now updated at sites 548 and 978.

2. Tracers of MOW derivates in the present and past Northeast Atlantic

2.1. Neodymium isotopes

Nd has an oceanic residence time of ~400–2000 years, slightly shorter than the global ocean mixing time (Arsouze et al., 2008; Rempfer et al., 2011). The dissolved Nd isotope composition of modern seawater in the Atlantic is controlled by weathering inputs of continental rocks of different ages and compositions, mixed and advected by water masses leading to ε_{Nd} values between −7 and −26 (cf. Frank, 2002) and thus serves as quasi-conservative tracer of water mass mixing and circulation (Supplementary text #1). For the unradiogenic Nd isotope signature of LSW (ε_{Nd} ~ −14) the input mainly stems from weathering of Precambrian rocks in Greenland and Canada and is dominated by the marginal exchange of downwelled waters with ice rafted, fluvial, shelf, and Eolian sediments (Lacan and Jeandel, 2005).

In contrast, modern MOW leaves Mediterranean Site 978 with an ε_{Nd} signature of −9.4 to −9.1 (Fig. 2b; Tachikawa et al., 2004). Farther downstream, ε_{Nd} signatures of MOW derivates become increasingly less radiogenic along its flow path through mixing with NACW and LSW. Combined evidence from various archives suggests that ε_{Nd} values change from −9.4 off southern Portugal (Stumpf et al., 2010) to −9.8 further west (Muiños et al., 2008), −11.1 to −11.2 in the Bay of Biscay (Rickli et al., 2009; Copard et al., 2011), and −10.5 at Site 548 west of Brittany (Khélifi et al., 2009). Finally, ε_{Nd} drops to −11.3 at Rockall Plateau Site 982 at 1135 m w.d. (this study) as compared to −12 to −13 characteristic of LSW below (Spivack and Wasserburg, 1988) and −13 of NAC above Site 982 (Lacan and Jeandel, 2004). Here, shallow intermediate waters on Rockall Plateau may even be less radiogenic with values as low as −14 (deep-sea coral ε_{Nd} data of Colin et al. (2010), Copard et al. (2010), and Robinson et al. (2014)). Thus, the ε_{Nd} difference between MOW and ambient Atlantic waters is sufficient to resolve changes in the past admixture of MOW in the Pliocene sediment records of sites 548 and 982. However, we note that Iceland–Scotland Overflow Waters at >1300 m depth near Rockall Plateau and volcanic-ash-contaminated sediments around Iceland also show seawater ε_{Nd} values of −9.7 to −10.3, similar to those of MOW derivates (Crocket et al., 2011; Elmore et al., 2011; Khélifi and Frank, 2014).

2.2. Estimates of salinity, temperature, density, and benthic $\delta^{13}C$

Elevated salinity (38.4 psu), temperature (13 °C), and density estimates (27.7–29) help us in tracing modern MOW across the northeast Atlantic (Figs. 1b and 6) and clearly exceed those of ambient water masses in the same depth range. For the Pliocene we need to consider two factors that may have dominated major changes in density and thus, changes in the reach and depth level of MOW:

(1) The initial density of MOW in the Strait of Gibraltar. Its variability depends on Mediterranean climate and the hydrological regimes that controlled intermediate and deep-water formation in the eastern and western Mediterranean. During the mid and late Pleistocene the density of MOW varied on millennial-time scales. It was particularly high during cold and arid Heinrich stadials (Zahn et al., 1997; Cacho et al., 2000; Voelker et al., 2006), a scenario that only started near the end of the Pliocene, with the onset of major Northern Hemisphere Glaciation ~2.8 Ma (Bartoli et al., 2006).
(2) Past changes in MOW injection were also controlled by changes in the aperture of the Strait of Gibraltar, today ~284 m deep and ~30 km wide (Bryden and Kinder, 1991), but strongly reduced

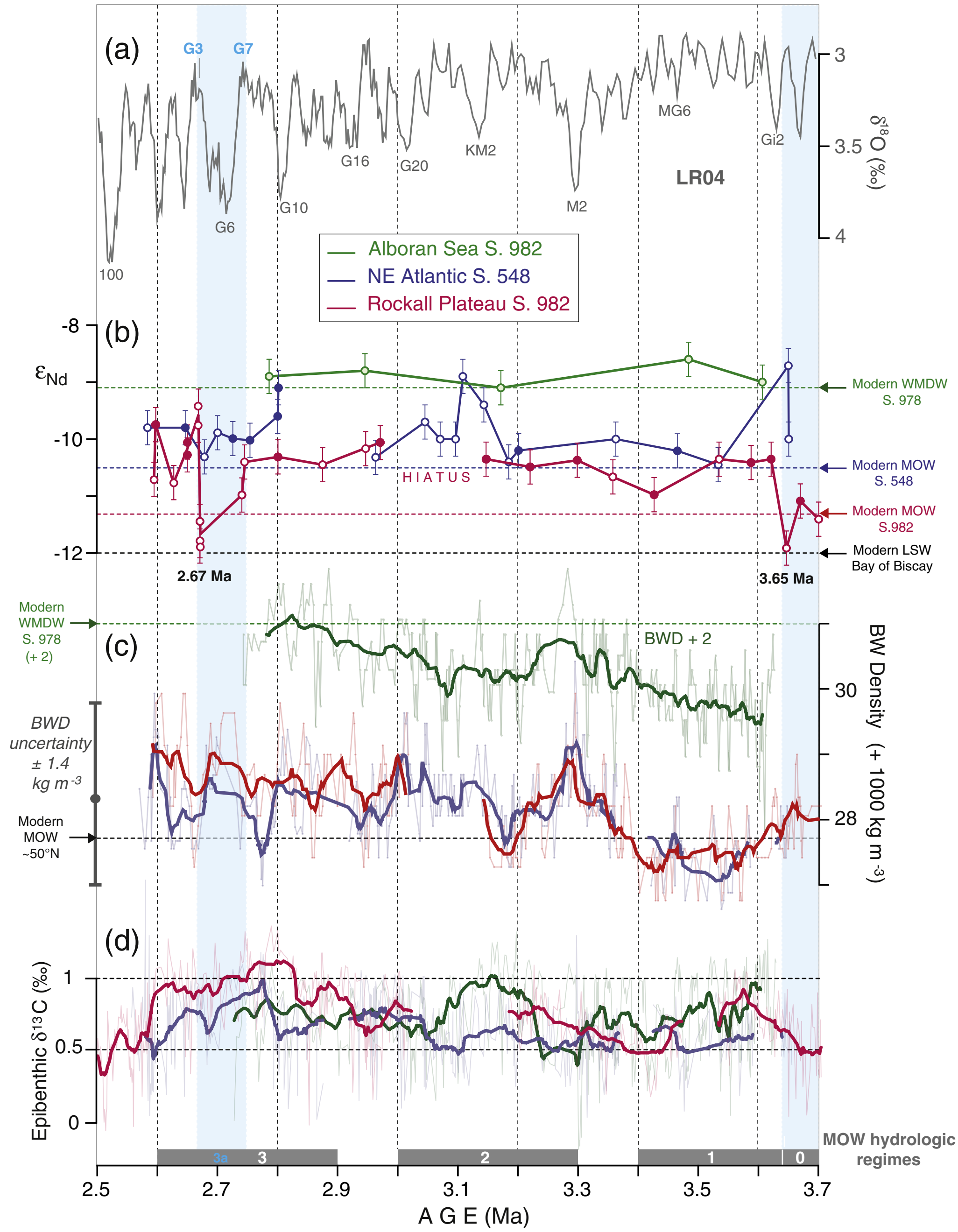

Fig. 2. Bottom water Nd isotope (ε_{Nd}) composition (b) at westernmost Mediterranean Site 978 (green) and northeast Atlantic sites 548 (blue) and 982 (red) versus age (Ma). Error bars correspond to 2σ external reproducibility. Full dots for sites 548 and 982 mark data from glacial, open dots data from interglacial sediments. Horizontal dashed lines indicate modern ε_{Nd} signals of Labrador Sea Water (LSW), Mediterranean Outflow Water (MOW), and Western Mediterranean Deep Water (WMDW) at the core locations under discussion. Data of sites 548 and 978 from 3.7 to 3.0 are from Khélifi et al. (2009). At sites 548 and 982 age control is based on correlation of the benthic $\delta^{18}O$ records, at Site 978 on correlation of the planktic $\delta^{18}O$ record to the global benthic $\delta^{18}O$ stack and marine isotope stage (MIS) numbers of LR04 (Lisiecki and Raymo, 2005) (a) (compare Supplementary Figs. S3a, b, and c). (c) Smoothed estimated bottom water density (BWD) curves and (d) epibenthic $\delta^{13}C$ records of Pliocene ventilation changes of West Mediterranean Deep Water (WMDW) at Alboran Sea Site 978 and Mediterranean Outflow Water (MOW) derivates at northeast Atlantic Site 548 and Site 982. Analyzed species are listed in Supplementary Table S1. Note the close coherence of BWD records of all three sites, in particular those of sites 548 and 982. Bars at the lower end of the figure show reach of MOW scenarios 0, 1, 2, and 3. Blue vertical bars mark hydrological scenarios 0 and 3a, when the influence of MOW derivates at Rockall Plateau was equal or weaker than today. (For interpretation of the references to color in this figure legend, the reader is referred to the web version of this article.)

during Pleistocene glacial sea level drops of ~130 m. Most likely, this bathymetric change was overcompensated by a rise in glacial Mediterranean aridity and evaporation and resulted in farther MOW penetration (Zahn et al., 1987). In contrast, the MOW flow may have been increased during Pliocene sea level highstands (Raymo et al., 2011; Miller et al., 2012; model experiments and synthesis in Rogerson et al. (2012)). However, little is known about changes in the aperture of the Strait of Gibraltar, controlled by geodynamics over the Pliocene.

The pronounced ventilation of Mediterranean deep and intermediate waters today results in $\delta^{13}C$ values of ~1.25–1.4‰ for MOW, significantly higher than those of nearby Atlantic intermediate waters (Zahn et al., 1987, 1997; Sarnthein et al., 1994), which unexpectedly contrast with 1.0 ± 0.05‰ measured in modern deep waters of the Alboran Sea (Pierre, 1999). During the last glacial cycle $\delta^{13}C$ values (up to 1.6‰) were elevated in deep waters of the Alboran Sea (Cacho et al., 2000). A similar trend was expected for Pliocene cooling periods on short and long time scales (Fig. 2d).

3. Materials and methods

3.1. Neodymium isotope analyses

The radiogenic Nd isotope composition of past bottom waters was extracted from leachates of authigenic Fe–Mn oxyhydroxide coatings of bulk sediment samples (Gutjahr et al., 2007). Different from the potential bias in other proxies based on stable isotope or element ratios, radiogenic Nd isotope ratios are not affected by biological processes. The analytical procedures employed to measure Nd isotopes are detailed in Supplementary text #1 (data deposited in the PANGAEA databank at http://www.pangaea.de).

3.2. Foraminifera species selected for proxy analyses

To reach an orbital to millennial-scale resolution of the proxy records (Supplementary Tables S1 and S2) 20 cm^3 samples of 2 cm thick sediment sections each were sampled at intervals of 10–20 cm at Site 978 and at intervals of 10 cm at sites 548 and 982. Oven-dried samples were disaggregated in H_2O_2 and wet-sieved at 63 μm. The coarse fraction was dried at 40 °C and sieved into 5 subfractions of >400 μm, 315–400 μm, 250–350 μm, 150–250 μm, and 63–150 μm. From the >250-μm fraction we picked planktic and benthic foraminifers for stable isotope and Mg/Ca analyses. The species selected are listed in Table S1. *Cibicidoides kullenbergi* is considered a junior synonym of *Cibicidoides mundulus* (van Morkhoven et al., 1986; details in Holbourn and Henderson, 2002). For minor element analyses we carefully checked all benthic specimens with regard to overgrowth while crushing them under the microscope. At Mediterranean Site 978 we used well-preserved glassy specimens only. Specimens at Atlantic sites 548 and 982 were not glassy, however, also without any sign of secondary calcite overgrowth.

3.3. Stable isotope analyses

Monospecific samples of 15–20 planktic and 3–5 benthic foraminifera specimens were gently crushed under the microscope and carefully ultrasonicated in ethanol for 30 s to separate fine-grained carbonate particles. After drying at 40 °C stable oxygen and carbon isotope compositions were measured on a Finnigan MAT251 mass-spectrometer connected to a Kiel I device at the Leibniz Laboratory for Radiometric Dating and Isotope Research of Kiel University. The $\delta^{18}O$ and $\delta^{13}C$ data are given relative to the Vienna PeeDee Belemnite (VPDB) standard. The analytical precision is ±0.07‰ for $\delta^{18}O$ and ±0.05‰ for $\delta^{13}C$. Benthic $\delta^{18}O$ values measured on *Cibicidoides* species were corrected for species-specific offsets relative to *Uvigerina peregrina* (+0.64), the oxygen isotope composition of which is in equilibrium with ambient sea water (Shackleton, 1974; Ganssen, 1983). Raw data are provided in Supplementary Figs. S1 and S2.

3.4. Mg/Ca analyses

At all sites investigated Mg/Ca ratios were measured on tests of *Cibicidoides mundulus* (analytical details in Supplementary text #2; raw data shown in Supplementary Figs. S1 and S2). Our Mg/Ca records are not corrected for potential changes in seawater Mg/Ca since it is spatially constant and has hardly changed on timescales of <1 Ma (Broecker and Peng, 1982). All sites of this study occur above the foraminifera lysocline, where dissolution is hardly affecting Mg/Ca. Also, we assume that our foraminiferal Mg/Ca values have not significantly suffered from changes in carbonate ion saturation. Modern northeast Atlantic waters are supersaturated with respect to calcite (Sosdian and Rosenthal, 2009). Moreover, Pliocene bottom waters were warmer and hence even more supersaturated (Gröger et al., 2003). Most importantly, BWTs (5°–16 °C) deduced in this study are warmer than 5 °C, the somewhat controversial cold end of the relationship between Mg/Ca and BWT (Yu and Elderfield, 2008). This does not apply to the onset of major NHG, when Site 548 was bathed in a MOW derivate <5 °C and carbonate ion saturation was possibly reduced for about 100 kyr (details farther below).

3.5. Alkenones as tracer of sea surface temperature

Sea-surface temperatures (SST) in the western Mediterranean Sea were derived from a record of C_{37} alkenone unsaturation ($U^{k'}_{37}$), using the technique of Prahl and Wakeham (1987) and the global field-based transfer equation of Conte et al. (2006) with a mean uncertainty of ±1.2 °C. This equation includes data from the Mediterranean and covers a broad SST range, and thus appears suitable for reconstructing high Pliocene SST in the Mediterranean Sea (details of alkenone analysis are provided in Supplementary text #4).

3.6. Derivation of bottom water temperature and salinity estimates

No temperature calibration has as yet been established for benthic Mg/Ca of *Cibicidoides mundulus* in the western Mediterranean Sea and northeast Atlantic at the water depths of MOW. To convert Mg/Ca data into estimates of BWT we used the global temperature equation defined for Mg/Ca of *Cibicidoides* sp. (Elderfield et al., 2006; details in Supplementary text #3). For Mediterranean Site 978 data we also used the equation of Lear et al. (2002), which also is defined for *Cibicidoides* species sensu lato, but mainly based on samples from Little Bahama banks with a temperature range extending to up to 18 °C. The temperature estimates of the two equations hardly differ. We preferred the equation of Elderfield et al. (2006), since it better constrains BWT below 5 °C. Also, we reduced the uncertainty range of low BWT estimates by increasing the number of replicates analyzed.

Using Mg/Ca-based BWT and epibenthic $\delta^{18}O$ we calculated the $\delta^{18}O$ signal of bottom waters ($\delta^{18}O_{bw}$) and estimates of bottom water salinity (BWS; details in Supplementary text #3). To extract estimates of past BWS, we corrected the benthic $\delta^{18}O_{bw}$ for the global ice volume effect, which was deduced from Pliocene $\delta^{18}O$ shifts in the LR04 record (Lisiecki and Raymo, 2005; Fig. 4) assuming that these shifts reflect ice volume changes only (0.1‰ = 10 m sea level). To calculate propagated errors of $\delta^{18}O_{bw}$ we employed the square root of the summed-up squared errors of BWT and benthic $\delta^{18}O$. Error bars in Figs. 3–5 were drawn for 10-/15-point running-averages of the records (Supplementary text #6).

In contrast, the $\delta^{18}O$ signal of surface waters, $\delta^{18}O_{sw}$, was rarely converted to actual equivalents of sea surface salinity (SSS). In the Alboran Sea $\delta^{18}O_{sw}$ and SSS changes mainly reflect changes in the local freshwater budget, and to a minor degree possibly changes in the salinity of inflowing Atlantic surface waters. However, this region lacks any transfer equation that properly calibrates local $\delta^{18}O_{sw}$ vs. SSS. A further problem may derive from the fact that SSTs of the near-surface habitat of *Emiliania huxleyi*, which carries the $U^{k'}_{37}$ signal, strongly differ from that of *Globigerinoides ruber* near 25 m depth, which carries the $\delta^{18}O$ signal. For calculating $\delta^{18}O_{sw}$ records (Fig. 4) we used $U^{k'}_{37}$-based annual SST estimates that only differ by ~2.5°–3.0 °C between the two different habitat depths. Indeed, this temperature difference applies to coeval foraminifera-based SST estimated for the Upper Pliocene at West Mediterranean Site 975 (Serrano et al., 2007). Moreover, we assume that surface-to-subsurface temperature anomalies have changed little over the Upper Pliocene and thus can be ignored. In our discussion we only refer to the prominent SSS minimum at 3.6 Ma and subsequent long-term SSS rise at 3.6–3.4 Ma, equivalent to >1.5 ‰ $\delta^{18}O_{sw}$ (i.e., an equivalent of ~7 °C). In comparison with other uncertainties, the problem of surface-to-subsurface temperature anomalies can be ignored.

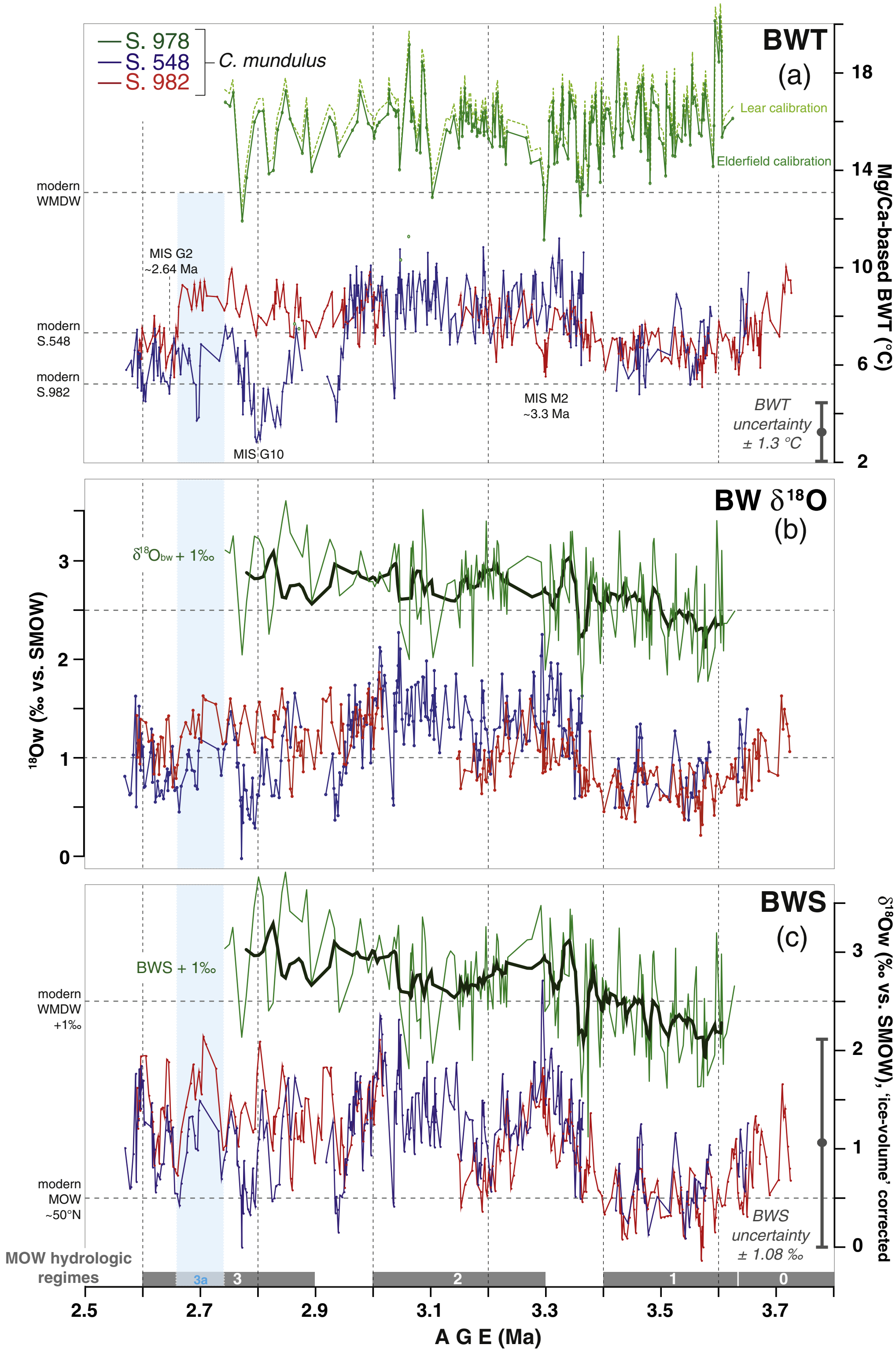

Fig. 3. Pliocene changes in (a) bottom water temperature (BWT), (b) $\delta^{18}O$ ($\delta^{18}O_{bw}$), and (c) 'ice-volume' corrected $\delta^{18}O_{bw}$ (=BW salinity) of Mediterranean Outflow Water (MOW) at northeast Atlantic sites 548 and 982 as compared to West Mediterranean Deep Water (WMDW) properties at Site 978 (note the shift of vertical scales), where ~20-kyr running means (thick lines) highlight long-term trends. Horizontal bars mark modern levels. BWT values are based on Mg/Ca ratios obtained from *Cibicidoides mundulus* (see Supplementary Figs. S1 and S2 and Table S1). Trend lines of BWT connect averages of paired and replicate measurements. Vertical bars give uncertainty range for single estimates of BWT and long-term changes in BWS and BWD (details in Supplementary text #6). MOW scenarios (0, 1, 2, and 3) are indicated at figure bottom.

3.7. Age control

For Alboran Sea Site 978, orbital stratigraphy was obtained from tuning the planktic $\delta^{18}O$ record to the stacked benthic $\delta^{18}O$ record LR04 (Lisiecki and Raymo, 2005). In contrast, the benthic $\delta^{18}O$ record of Site 978 does not reflect the evolution of global ice volume change, since it is dominated by Mediterranean deep-water formation (Supplementary Fig. S3a). Furthermore, our Site 978 age model 3.62–2.72 Ma

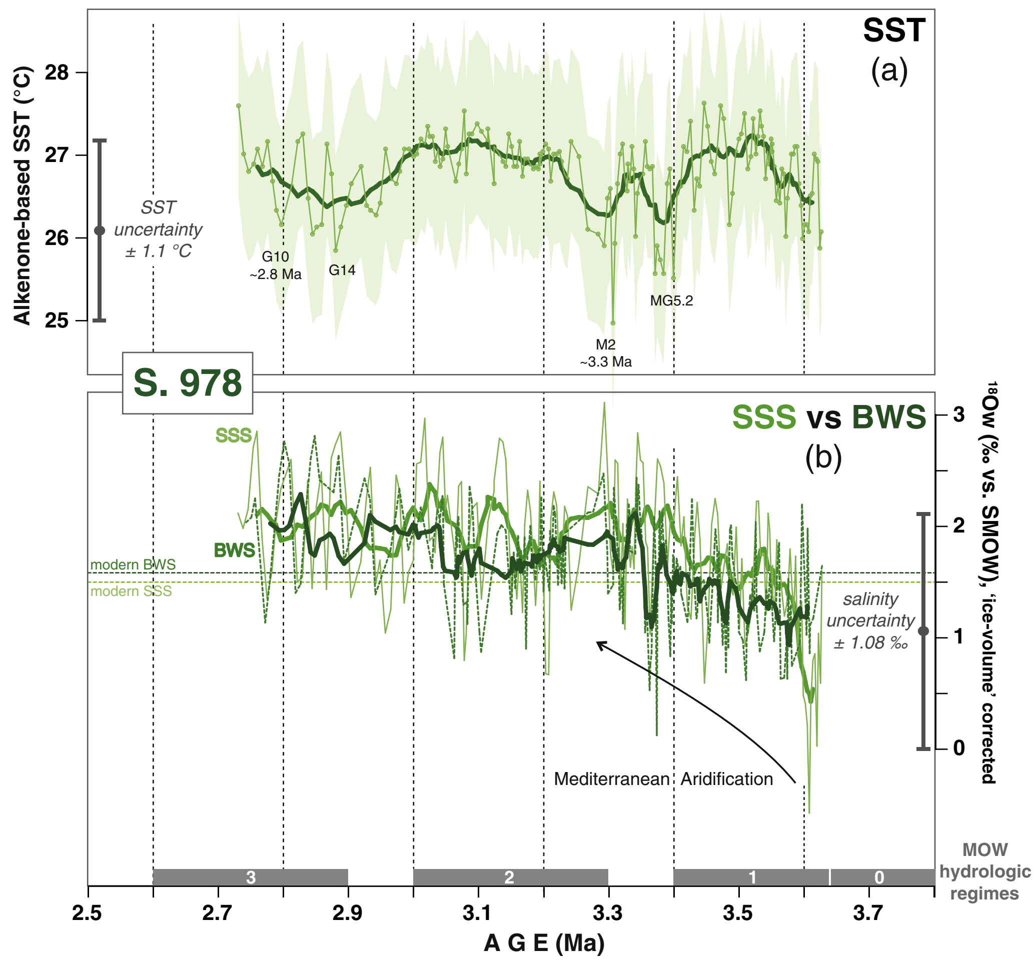

Fig. 4. Changing sea-surface and bottom water properties at West Mediterranean Site 978. $\delta^{18}O$ is measured on *Globigerinoides ruber*, *Globigerina bulloides*, and *Globigerinoides obliquus* (see Supplementary Fig. S3a and Table S1). Horizontal lines show modern levels. MOW scenarios (0, 1, 2, and 3) are indicated at the bottom of the figure. The labeled arrow marks a major long-term trend. SSS = sea-surface salinity; SST = sea-surface temperature; BWS = bottom-water salinity. Vertical bars give uncertainty range for single estimates of SST, SSS, and BWS (details in Supplementary text #6).

integrates evidence from shipboard bio- and magneto-stratigraphy (Leg 161 Shipboard Scientific Party, 1996) (Supplementary Table S2). Some core breaks have led to a sediment loss equal to an interval of up to 12,500 years (Fig. S3a). Planktic and benthic $\delta^{18}O$ records are based on foraminifera species listed in Supplementary Table S1. Sedimentation rates and sampling intervals are listed in Supplementary Table S2.

Likewise, the Site 548 age model is based on orbital tuning of the planktic $\delta^{18}O$ record (Fig. S3b) and incorporates evidence from shipboard bio- and magnetostratigraphy (Leg 80 Shipboard Scientific Party, 1985; Supplementary Table S2), covering the interval 3.68–2.56 Ma. The sediment record of Site 548 suffers from three hiatuses, as consequence of which parts of Marine Isotope Stage (MIS) G13 to G15, KM2 to KM3, and MG4 were lost. Further small sediment sections may have been lost at core breaks near MIS G20, M2, and Gi2. Here, sampling gaps may reach 7900 to 32,000 years (Supplementary Fig. S3b). The planktic and benthic $\delta^{18}O$ records are based on species listed in Supplementary Table S1. Sedimentation rates and sampling intervals are listed in Supplementary Table S2.

As for sites 978 and 548, the age model of Site 982 benthic $\delta^{18}O$ records was tuned to the orbital oscillations of reference record LR04 (Lisiecki and Raymo, 2005; details in Khélifi et al., 2012). In particular, our age model is based on a renewed hole-specific inspection of magneto-stratigraphic reversals (Channell and Guyodo, 2004) and includes new epibenthic $\delta^{18}O$ records for short Pliocene sediment sections supplemented for holes 982A, B, and C. These sections cross core breaks in the $\delta^{18}O$ record first published for Hole 982B (Venz and Hodell, 2002; Lisiecki and Raymo, 2005). The age model of Khélifi et al. (2012) for the composite $\delta^{18}O$ record results in a hiatus, during which the Kaena magnetic subchron was lost, and in an absolute-age reduction by 20–130 kyr for all proxy records over the time span 3.2–2.7 Ma (Supplementary Table S2, Supplementary Fig. S3c). The planktic (unpubl. data) and benthic $\delta^{18}O$ records were measured on species listed in Supplementary Table S1. Supplementary text #5 details arguments that refute the stratigraphic view of Lawrence et al. (2013).

4. Results

4.1. Overview of Pliocene ε_{Nd} records (Fig. 2b)

At West Mediterranean Site 978, WMDW, a major source of MOW, showed a stable ε_{Nd} signature of −9.1 to −8.6 from 3.6 to 2.75 Ma, which is slightly (0.5 units) more radiogenic than ε_{Nd} values of −9.4 to −9.1 found for deep waters at West Mediterranean sites today (Tachikawa et al., 2004). At northeast Atlantic Site 548 ε_{Nd} signatures ranged between −10.5 and −9.7 from 3.65 to 2.58 Ma, as compared to −10.5 today. At 3.65, 3.1, and 2.8 Ma short orbital-scale ε_{Nd} excursions reached −9.1 to −8.7, values similar to those of modern MOW source waters at Site 978 (Fig. 2b top).

Likewise, distal Site 982 showed a relatively stable ε_{Nd} signature of −11 to −9.3 for the same period of time (Fig. 2b base). In total, the Pliocene signatures were 0.5–1.3 units higher than the modern, less

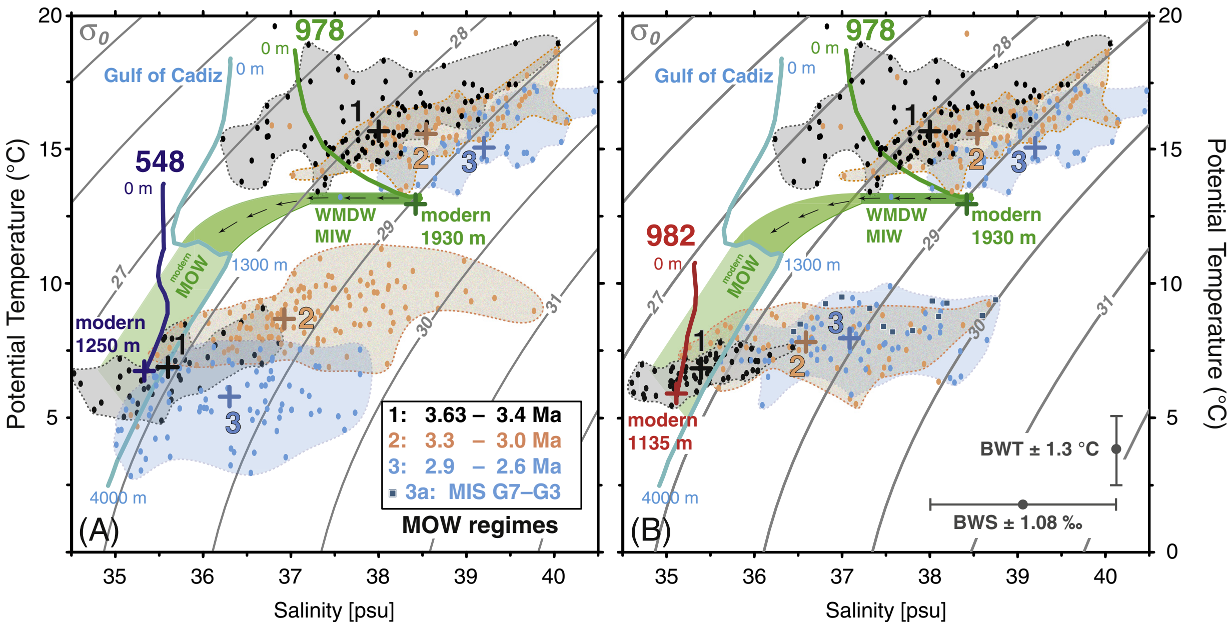

Fig. 5. Temperature/salinity/density plots for West Mediterranean Deep Water (WMDW) at Alboran Sea Site 978 and Mediterranean Outflow Water (MOW) at northeast Atlantic sites 548 and 982. Thin solid curves are isolines of equal density (numbers are kg m^{-3} − 1000). Temporal shifts in average BWT and BWS of MOW amongst three/four major scenarios are compared to coeval changes in WMDW. '+' signs present averages of hydrologic regimes 1–3 as listed in Table 1. Age ranges of MOW scenarios 0, 1, 2, and 3 are given at lower left. Vertical and horizontal bars at lower right give uncertainty range for long-term changes in BWT and BWS (details in Supplementary text #6).

radiogenic ε_{Nd} range of −11.6 to −10.9 ± 0.3 found in triplicate for two different core top samples in our laboratory. In contrast, Late Holocene deep-sea coral data from sites closely above Site 982 show seawater ε_{Nd} signatures of −12.9 to −14.2, which either suggest an influence of LSW or one of deep-reaching NAC (Colin et al., 2010; Copard et al., 2010; Robinson et al., 2014). After all, we conclude that the Pliocene ε_{Nd} data of Site 982 reliably reflect MOW-derived bottom water signatures that were not influenced by partial dissolution of volcanic ashes from Iceland, in contrast to ε_{Nd} data at Site BOFS17K ~40 nm farther northwest on Rockall Plateau, more proximal to Iceland (Elmore et al., 2011). Also, the ε_{Nd} signal was not controlled by Norwegian Sea overflow waters (Lacan and Jeandel, 2004), that pass by the top of Rockall Plateau few hundred meters below Site 982 because of higher density (Fig. 1, lower panel). In particular, we regard it as highly unlikely that volcanic ash supply has continuously induced a more radiogenic ε_{Nd} signature at Site 982 over the complete time span 3.6–2.8 Ma. In addition, deep-sea coral ε_{Nd} data from the nearby Porcupine Sea Bight (Montero-Serrano et al., 2011) show that intermediate waters in the eastern North Atlantic have been extremely variable in the past and shifted from ε_{Nd} values as radiogenic as −9.5 at 280 ka to −15 in the early Holocene depending on the different source areas of waters entrained in the North Atlantic.

Both the initial ε_{Nd} signature of WMDW at Site 978 and that of MOW derivates in the northeast Atlantic were slightly higher during the late Pliocene than today. The ε_{Nd} record of Site 982 was up to ~0.8 units less radiogenic than that of more proximal Site 548. This reflects progressive dilution of the Mediterranean ε_{Nd} signal by LSW (possibly also by NAC) along its flow path to the north, similar to today. MOW signatures (−9 to −10.5 at Site 548 and −10 to −10.5 at Site 982) were persistently more radiogenic than those of LSW (−11 to −12; Site 3511-1; Muiños et al., 2008). Thus, most likely no intermediate waters other than MOW had an ε_{Nd} signature positive enough to produce the relatively radiogenic values found at our two core sites in the Pliocene North Atlantic, in particular at Site 548. ε_{Nd} records of northeast Atlantic sites 548 and 982 suggest a largely stable Pliocene advection of MOW at essentially constant water depths from the Alboran Sea up to Rockall Plateau. From 3.7 to 3.64 and from 2.75 to 2.67 Ma, however, ε_{Nd} values at Site 982 dropped down to −11 to −12 each, excursions that either reflect an enhanced advection of LSW and/or a deepening of the NAC waters, thus a short-lasting cessation or major shoaling of the MOW plume.

A potential admixture of Antarctic Intermediate Water (AAIW) to MOW is hard to specify at northeast Atlantic margin sites, since modern AAIW is already highly diluted, when it reaches locations off Portugal (~13 ± 8%; Louarn and Morin, 2011). The progressive dilution of AAIW results in a meridional ε_{Nd} gradient from −11 at 10°N (von Blanckenburg, 1999) to −11.7 at 22°N (Rickli et al., 2009) and hence, in an ε_{Nd} signature hard to distinguish from that of LSW.

These conclusions still apply, when taking into account a general ~1 ε_{Nd} shift of deep water signatures to more radiogenic values in the western and eastern North Atlantic at 700–2700 m depth in the late Pliocene as indicated by low-resolution time series of ferromanganese crusts (O'Nions et al., 1998). Others that were measured within the water depth of modern LSW in the Bay of Biscay stayed essentially constant near ε_{Nd} = −11 (Muiños et al., 2008). Although the locations of the ferromanganese crusts are not fully representative for tracing of Pliocene LSW close to our two sediment sites, the latter ε_{Nd} signature confirms that MOW derivates indeed did not reach distal Site 982 anymore both at 2.8–2.6 and 3.7–3.64 Ma. In summary, given that the original ε_{Nd} signature of Pliocene LSW that was slightly more radiogenic than that of modern deep waters, we consider an ε_{Nd} signature of −11 to −12 a realistic Pliocene end member value for LSW. Future sedimentary ε_{Nd} records of NADW, LSW, and NAC will help us to confirm this estimate.

4.2. Benthic $\delta^{13}C$ records (Fig. 2d)

At Site 978 the epibenthic $\delta^{13}C$ record of Pliocene Mediterranean deep-water ventilation shows spectacular short-term oscillations between 0 and 1.5‰, that clearly follow the 21-ky cycle of orbital precession, with $\delta^{13}C$-based ventilation minima being largely confined to interglacial stages (Supplementary Fig. S4). Long-term $\delta^{13}C$ maxima of >1‰ occurred both prior to 3.6 Ma and at 3.23–3.08 Ma. In general, Pliocene source waters of MOW were much less ventilated than those during the late Pleistocene (Cacho et al., 2000; Voelker et al., 2006). Likewise, δ^{13}C-based ventilation of Pliocene MOW was clearly reduced at East Atlantic margin Site 548 (running average of 0.5–1.0‰ vs. 1.0–1.7‰ during Pleistocene cold stages; Sarnthein et al., 1994). The δ^{13}C record of Site 982 shows a distinct long-term increase in bottom water ventilation by ~0.3‰ from 3.45 to 3.25 Ma, when rising BWT and BWS suggest a major intensification of MOW flow (see below). After 2.9/2.8 Ma, δ^{13}C records of sites 548 and 982 display a prominent synchronous maximum that paralleled the onset of major NHG around MIS G10–G4 (Sarnthein et al., 2009), followed by a long-term drop from 2.7 to ~2.5 Ma, trends without analogy in the δ^{13}C record of Mediterranean Site 978. Different from the Pleistocene (Venz and Hodell, 2002), Pliocene δ^{13}C values at Site 548 generally were ~0.2‰ lower than those at more distal Site 982, probably the result of highly ventilated waters admixed via North Atlantic intermediate and/or NAC waters that dominated over MOW.

4.3. Variations in bottom water temperature and salinity

At West Mediterranean Site 978 the BWT of modern MOW source waters is 13 °C, BWS is 38.4 psu, and bottom water density (BWD) is 1029 kg m^{-3} (NODC, 2001). From 3.6 to 2.7 Ma Mg/Ca ratios were on average 5.5 and rarely reached 7.5–8.0 mmol mol^{-1} (Fig. S2), which translates to Pliocene BWT of ~15°–6 °C, rarely even 18 °C, and thus BWT 2°–5 °C warmer than today (Fig. 3a). In addition, the BWT record shows many short-lasting cold oscillations down to 14 °C and below, possibly following 20-ky and 95-kyr orbital cycles (for uncertainty ranges see Supplementary texts #3 and #6).

Average ($\delta^{18}O_{bw}$-based) BWS at Site 978 showed a unique minimum near 3.55–3.6 Ma, ~0.5‰ $\delta^{18}O_{bw}$ or 1.0 psu lower than today (Fig. 3b and c). This minimum was accompanied by a major freshening of the surface waters by ~2 psu compared to today (Fig. 4). From 3.55 to 3.3 Ma, salinities of both surface and bottom waters rose by ~1‰ $\delta^{18}O_w$ or ~2 psu, a shift that exceeds the uncertainty range of individual estimates and that of the data populations averaged for MOW Regimes 1 and 2 (Figs. 2c and 5; see Table 1 and details farther below). From 3.2 to 3.05 Ma, average BWS dropped back to the modern level. After a renewed rise by ~0.8 psu near 3.05 Ma BWS stayed generally high until 2.75 Ma, except for short-term minima at warm MIS G17, G13, G11, and G7(~2.96, 2.86, 2.83, and 2.77 Ma).

At Site 548, the modern BWT of the lowermost part of MOW is 7.5 °C, BWS is 35.5 psu, and BWD is 1027.74 kg m^{-3} (Shipboard Scientific Party, 1985). As documented by Khélifi et al. (2009), BWT showed a long-standing minimum from 3.6 to 3.45 Ma. Subsequently, they rose from 6° to ~10 °C until 3.33 Ma and subsequently oscillated at 8°–11 °C until MIS G17 (2.95 Ma) (Fig. 3a). Immediately after 2.95 Ma, average BWT underwent a unique abrupt and long-standing drop by 3°–4 °C down to ~4 °C at MIS G16, an immense shift little understood as yet. After 2.8 Ma, average BWT returned back to 6.5°–7.5 °C and thus to temperatures only slightly lower than those of today.

Pliocene BWS largely varied closely in parallel with changes in BWT such as (i) at 3.45–3.33 Ma, where average $\delta^{18}O_{bw}$ showed a unique rise by 0.7–1.0‰ equal to ~1.4–2.0 psu BWS, (ii) a long-lasting high in BWS oscillations from 3.33 to ~3 Ma, and (iii) at MIS G16 (after 2.96 Ma), where BWS decreased by almost 3 psu (~1.5‰ $\delta^{18}O_{bw}$) until 2.93 Ma (Fig. 3b, c). Subsequently, BWS oscillated with large amplitudes between 0 and up to 2 psu above the modern level.

Today, Rockall Plateau Site 982 (5.5 °C, 35 psu, ~1027.6 kg m^{-3}) is bathed in upper NADW (i.e. LSW) with minor derivates of distal MOW admixed (Fig. 1; McCartney and Mauritzen, 2001). In the late Pliocene both the long-term trends and absolute level of BWT and BWS at Site 982 closely matched those of MOW-dominated Site 548 (Fig. 3a–c). This applies, for example, to the major rise in BWT and BWS from 3.45 to 3.3 Ma that ended with a salient maximum 3.3 Ma (MIS M2), and to essentially synchronous BWT and BWS oscillations between 3.25 and 2.95 Ma. However, the records of sites 982 and 548 began to deviate at the onset of major NHG, 2.95–2.65 Ma, when BWT of Site 548 started to oscillate at levels ~2–4 °C lower than that at Site 982. Here, a long-term drop in BWT by 2–3 °C only occurred at MIS G2 (~2.65 Ma), almost 300 kyr after that of Site 548. Subsequently, BWT (and BWS) records of both sites again matched as closely as prior to 2.95 Ma, however, at a temperature level that stayed significantly higher than that of today (Fig. 3).

5. Discussion

5.1. Long-term changes in the advection, reach, and progressive dilution of MOW

The present study is centered around the question of whether derivates of the outflow of Mediterranean Sea Water have reached up to Rockall Plateau during the late Pliocene as MOW eddies sporadically do today. ε_{Nd} signatures at northeast Atlantic Site 982 (Fig. 2b) that are more radiogenic than those in other intermediate water masses below and above suggest that the answer in fact is yes, though not for the complete but for most of the time period analyzed. A further objective deals with the forcings that may have influenced Pliocene long-term major changes in the advection of MOW under climate boundary and sea level conditions very different from today. By now, Pliocene changes in the MOW plume received little attention, except for rare pioneer studies of Loubere (1987a, 1987b, 1988) and Khélifi et al. (2009) and various reports on the Pliocene evolution of oceanography and climate within the Mediterranean region, recently summarized by Colleoni et al. (2012) and Rogerson et al. (2012).

Our prime evidence is based on the new ε_{Nd} record of Site 982. It shows a relatively constant radiogenic Nd signature only interrupted by two marked excursions toward less radiogenic values (Fig. 2b) reflecting two periods of time, one prior to 3.63 and one from 2.75 to 2.65 Ma, when MOW did not reach Rockall Plateau any longer (hydrologic regimes 0 and 3a; Figs. 2b, c, and 5). Further evidence is based on long-term major changes in BWT and BWS between 3.63 and 2.6 Ma (Figs. 3–5). These enable us to distinguish a total of three major long-term stable hydrological regimes prevailing over the periods of time 3.63–3.4 Ma, 3.3–3.0 Ma, and 2.9–2.6 Ma, listed in Table 1, which likewise resulted from differences in flow strength, lateral mixing and progressive dilution of MOW. Each regime is defined by a very broad temperature–salinity array (Fig. 5). Their average values listed in Table 1 only represent a coarse approximation. At Mediterranean Site 978 the three regimes only differ little but in a gradual shift in BWS. In contrast, at Site 548 the Regimes 1, 2 and 3 differed significantly by offsets in both BWS and BWT. At Site 982 strongly reduced BWS clearly distinguish Regime 1 from the overlapping arrays of Regimes 2 and 3. Within Regime 3 the short-lasting event of Regime 3a stands out by a significant rise in BWT.

As displayed by the schematic transects of Fig. 6 and Table 1, vertical shifts in the MOW plume between Gibraltar and Rockall Plateau were mainly driven by changes in both the density of MOW and that of North Atlantic intermediate and NAC waters. During scenario 0 (prior to 3.63 Ma; not documented at Site 978 and hardly at Site 548) an excursion to extremely low ε_{Nd} signatures and fairly low equivalent values of BWS and BWS suggests that – different from today – no MOW derivates penetrated up to Rockall Plateau. During Regime 1, equivalents of bottom water salinity and density at West Mediterranean Site 978 initially were slightly lower than today. By and large, the initial salinity low matched a similar extreme low in sea surface salinity (Fig. 4), and hence probably resulted from initially still enhanced humidity of Mediterranean climate (Khélifi et al., 2009). In turn, the West Mediterranean low in BWS and BWD must have weakened the flow of MOW and have led to a reduction of salinities and densities of MOW at sites 548 and 982, down to a level similar to today (Figs. 2 and 4).

Table 1
Average estimates for bottom water salinity (BWS) and density (BWD) at sites 978, 548, and 982, displayed for various hydrologic regimes of the Pliocene as defined in the text, Section 5.1.

Hydrological	West Mediterranean		North East Atlantic			Rockall Plateau		
Regime	Site 978		Site 548			Site 982		
	Ø BWS (psu) ± 0.4	Ø BWD kg m−3 ± 1.4	Ø BWS (psu) ± 0.3	Ø BWD ±0.6 kg m−3	Ø ε_{ND} ±1.4	Ø BWS (psu) ± 1.4	Ø BWD ±0.3 kg m−3	Ø ε_{ND} ±0.3
Today	38.4	1029.0	35.5	1027.74	−10.5	35.0	1027.6	−11.3
3a (2.75–2.65 Ma)	–	–	37.0?	1029?	–	37.5	1028.9	−11.5
3 (2.95–2.6 Ma)	39.2	1029.2	36.3	1028.6	−9.9	37.1	1028.9	−10.6
2 (3.3–3.0 Ma)	38.5	1028.7	36.95	1028.7	−9.8	36.6	1028.6	−10.4
1 (3.63–3.4 Ma)	37.4	1028.2	35.5	1027.9	−9.8	35.0	1027.7	−10.5
0 (>3.63 Ma)	Extreme minimum?				–	35.5	–	−11.6

However, ε_{Nd} signatures at Site 982 already were clearly more radiogenic during Regime 1 than today (−10.5 versus −11.3). Consequently, some derivates of MOW must then have reached Rockall Plateau Site 982 and possibly formed an admixture to NAC and/or LSW stronger than today.

The transition between Regimes 1 and 2, 3.4–3.3 Ma, was marked by a major rise in salinity and density of both Mediterranean deep waters and MOW (Table 1), which indicates an enhanced MOW advection that culminated near 3.3 Ma. The origin of this increase in MOW flow and a final overshoot were assigned to a prominent rise in Mediterranean summer aridity yet unexplained (Khélifi et al., 2009; pollen and lake-based evidence of reduced African summer monsoon in Fauquette et al. (1998) and Drake et al. (2008)). Benthic $\delta^{13}C$ data (Fig. 2d) suggest that this rise has caused a major increase in deep-water ventilation at Rockall Plateau Site 982. High bottom water densities continued to prevail at sites 548 and 982 over subsequent Regime 2, ~1 kg m^{-3} higher than today, while density estimates at Site 978, the source region of MOW, stayed slightly lower than today (Fig. 5). Hence, the density gradient between Mediterranean Sea and Rockall Plateau had largely disappeared (Table 1). During this time we surmise that the MOW plume expanded by up to ~500 m to greater water depths (Fig. 6).

Hydrological Regime 3 started immediately after MIS 17, 2.95 Ma, with an abrupt 5-degree drop in BWT at Site 548 (Fig. 3), which, however, was not reflected at Site 982, but coincided with a marked increase in bottom water ventilation at Site 982, that lasted until ~2.6 Ma (Fig. 2d). Both events were coeval with the onset of the final closure of the Central American Seaways, which most likely finally triggered the onset of major NHG (Bartoli et al., 2005; Sarnthein et al., 2009). We conclude that this major event also induced the major changes in both the Mediterranean Outflow and Atlantic Meridional Overturning Circulation observed at the boundary between hydrologic Regimes 2 and 3. Typical for cold stages in the Pleistocene (Zahn et al., 1997), BWD at Mediterranean Site 978 increased up to values slightly higher than today, whereas BWD at Atlantic sites 548 and 982 persisted at the high levels already reached during Regime 2 (Table 1), no matter, whether Site 982 was bathed in derivates of MOW or in pure Atlantic waters (Fig. 5).

During Regime 3a, 2.75–2.65 Ma, high BWD values at Site 982 coincided with a significant warming of BWT by to 2°/3 °C (Figs. 3 and 5), when ε_{Nd} signatures (Fig. 2b) suggest that MOW fully disappeared from Rockall Plateau. We think that it is unlikely that cold LSW then replaced the MOW at Rockall Plateau. Instead we assume that waters with more negative ε_{Nd} values were admixed from the overlying warm, and then clearly intensified NAC (Sarnthein et al., 2009). Also, the MOW plume may have weakened hence shifted upslope (Fig. 6). We may speculate that the ultimate trigger of Regime 3a was linked to the major sea-level drop by >20 m for interglacial stages over MIS G17–G3 (Miller et al., 2012). This drop implies a significant restriction in the aperture of the Strait of Gibraltar gateway from ~2.95 to 2.72 Ma, which resulted in a reduced and thus likely shallower injection of Mediterranean waters at the level of the North Atlantic intermediate water circulation. In agreement with the ‘firehouse principle’ the consequences of this shift were most obvious at distal Site 982.

In comparison with hydrological Regime 3a the breakdown of MOW advection outlined for Regime 0 (>3.63 Ma) may have been different. In the mid Pliocene global sea level was high and did not restrict the aperture of the Strait of Gibraltar. Moreover, the bottom waters that replaced MOW displayed only minor warming, whereas $\delta^{13}C$-based estimates showed an extreme ventilation minimum (Figs. 2d and 3). Different from Regime 3a, the boundary conditions of Regime 0 may indicate an intrusion of LSW up to the top of Rockall Plateau, which had been poorly ventilated during the late Pliocene (Bartoli et al., 2005).

5.2. Changes in MOW salt discharge as potential trigger of changes in Atlantic MOC

Reid (1979) used conceptual models and observations to postulate that MOW-based discharge of heat and salt may reach the Nordic Seas, where any increase in salinity may trigger enhanced NADW formation which in turn may contribute to global climate change. So far, Reid's hypothesis has hardly been tested by paleoceanographic records (McCartney and Mauritzen, 2001; Bower et al., 2002).

On the other hand, model simulations yielded controversial results on the role of MOW-borne salt discharge. New et al. (2001) concluded that MOW does not penetrate beyond Rockall Plateau at 53°N and thus cannot directly inject any salt into the cells of deep-water formation in the Nordic Seas, but only indirectly admix salt to NAC waters from below. Rahmstorf (1998) reasoned that the injection of MOW salt may at best enhance NADW formation by ~1 Sv, which is much less than the seasonal and interannual fluctuations of the flow of NADW amounting to ~18 ± 7 Sv (Frajka-Williams et al., 2012). In contrast, Hecht et al. (1997), Price and Yang (1998), and Wu et al. (2007) ascribed a more positive role to MOW in maintaining AMOC, which accordingly might slow down by as much as 15% without MOW. In turn, Bigg and Wadley (2001) postulated an enhanced influence of MOW on AMOC intensity for glacial periods.

To better constrain the potential role of MOW-borne salt, we compare the two most prominent late Pliocene changes in the flow of MOW established in this study with the coeval evolution of NADW ventilation as a reflection of AMOC intensity. In summary, the evidence

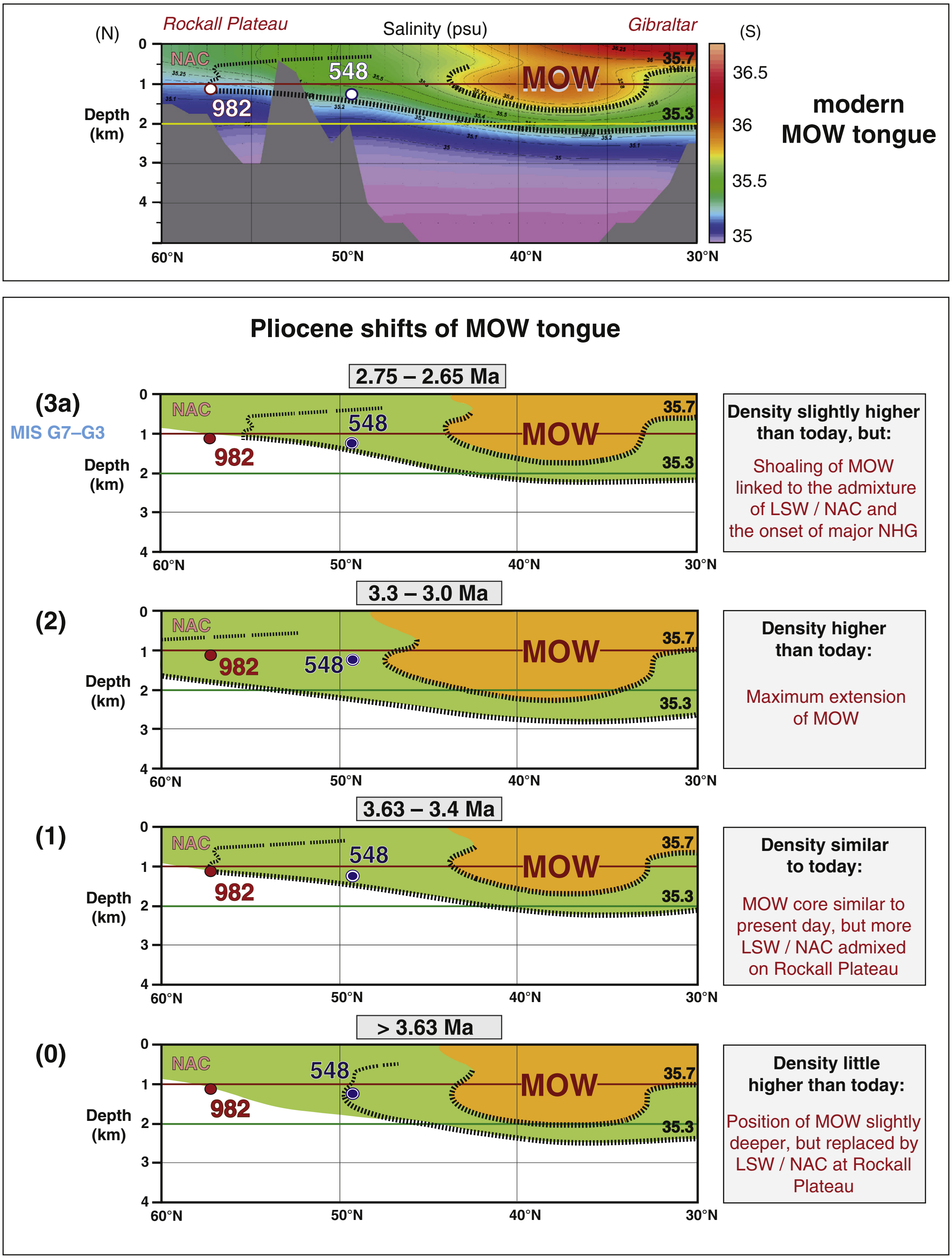

Fig. 6. Schematic reconstruction of four Pliocene hydrologic regimes (~3.7–2.65 Ma) at sites 548 and 982 to outline past changes in the depth and extent of the Mediterranean Outflow Water (MOW) plume (indicated by two dotted lines) along the northeast Atlantic continental margin as compared to the modern spread of MOW (Ocean Data View; top panel; NODC, 2001, and Schlitzer, 2013). Shifts in the reach and vertical position summarize evidence from temporal and lateral changes in bottom water ε_{Nd} (Fig. 2b) and density signatures (Fig. 5), moreover from δ^{13}C-based estimates of bottom water ventilation (Fig. 2d). Average salinity isolines of 35.3 and 35.7 psu (compare Table 1) facilitate comparison between the Pliocene time slices and their modern analog. LSW = Labrador Sea Water. NHG = Northern Hemisphere Glaciation.

from our data does not support the Mediterranean salt hypothesis of Reid (1979).

First, the distinct minimum in MOW injection around 3.65 Ma (Fig. 6, Regime 0) did not lead to any visible reduction in AMOC intensity (Ravelo and Andreasen, 2000). Later, the most prominent 1.5-psu rise of MOW salinity from 3.5 to 3.3 Ma (Fig. 5; Scenario 1–2 transition) likewise did not translate into any significant rise of lower NADW production. The ventilation record of mid-Atlantic ridge Site 607 (3427 m w.d.; Kleiven et al., 2002) was not affected at all. Only much later after 3.2 Ma, a minor 0.25‰ rise in δ^{13}C marked a slight increase in bottom water ventilation. We only know of a single potential linkage between NADW composition and this most distinct MOW density rise in the late Pliocene, which is a modest rise in coeval upper NADW ventilation by <0.25‰ $\delta^{13}C$ at Site 999 (2828 m w.d.) in the Caribbean Sea which is filled by upper NADW only (Haug and Tiedemann, 1998). In contrast, contemporaneous ventilation did not increase at far distal NADW sites 704 (2532 m w.d.) and 1092 (1976 m w.d.) in the southern South Atlantic (Andersson et al., 2002). In summary, we cannot completely rule out any role of strongly increased MOW salt advection on the formation of upper NADW, in particular during periods of decreased AMOC. However, presently available evidence suggests that the intensity of middle and lower NADW formation remained largely unaffected.

6. Conclusions

Combined sediment records of radiogenic Nd isotopes (ε_{Nd}) and of ventilation, temperature, salinity, and derived density changes in bottom waters at West Mediterranean Site 978 and northeast Atlantic margin sites 548 and 982 document the late Pliocene history of changes in the original composition, advection, and progressive dilution of Mediterranean Sea Waters (MOW) in the northeast Atlantic. On the basis of these data we define four hydrologic regimes and draw the following conclusions:

1. ε_{Nd} signatures show that MOW derivates reached from Gibraltar up to Rockall Plateau over most of the late Pliocene, from 3.6 to 2.75 Ma and once more, after 2.65 Ma, but not from 3.75 to 3.6 and from 2.75 to 2.65 Ma (Regimes 0 and 3a), when the flow of MOW decreased significantly.
2. From 3.6 to 3.45 Ma (Regime 1) bottom water salinities and densities of MOW were low and then increased by ~1.5 psu and 1 kg m^{-3}, respectively, between 3.45 and 3.3 Ma, coeval with a long-term warming of bottom waters both at sites 548 and 982. This transition between Regimes 1 and 2 documents a major and long-term intensification of MOW advection and probably resulted in a lowering of the MOW plume by ~500 m.
3. This enhanced flow of MOW matched a clear rise in bottom water salinity and density of West Mediterranean deep waters and a rise in sea surface salinity (Khélifi et al. 2009). These trends suggest strongly enhanced deep-water convection in the Mediterranean Sea, which was driven by increased aridity of Mediterranean summers and in turn, by a reduction in African summer monsoon intensity as also suggested by pollen records.
4. The increased injection of MOW into the North Atlantic induced a distinct rise in epibenthic $\delta^{13}C$ reflecting enhanced bottom water ventilation at Rockall Plateau Site 982. However, this did not translate into any significant strengthening of NADW ventilation and hence provides little support for the hypothesis that a rise in MOW advection may foster North Atlantic Meridional Overturning Circulation.
5. Immediately after 2.95 Ma, our records of MOW show massive changes that mark the onset of Regime 3, suggesting a linkage to the onset of major Northern Hemisphere Glaciation. In particular, we see long-term drops in bottom water temperature and (less obvious) salinity at Site 548 slightly later followed by a culmination in bottom-water ventilation both at sites 982 and 548 from 2.85 to 2.72 Ma. However, no correlative changes occurred at Mediterranean Site 978. Finally, less radiogenic ε_{Nd} signatures document a temporary disappearance of MOW derivates at Rockall Plateau, the distal end of the MOW plume (Regime 3a) and enhanced entrainment of NAC waters. This event was possibly tied to a drop of the Mediterranean outflow due to major glacial sea-level lowering that led to a reduced aperture of the Gibraltar gateway.

Acknowledgments

We acknowledge Wolfgang Kuhnt, Uwe Pflaumann, and Ann Holbourn for valuable advice with foraminiferal species definition. Valuable suggestions of three reviewers helped us to streamline our manuscript. Birgit Schneider assisted with Ocean Data View. Roland Stumpf and Anne Osborne helped with sample leaching. Karin Kissling and Claudia Teschner helped with ICP-OES and MC-ICPMS analyses. Silvia Koch assisted with the extraction of Alkenones. Thomas Blanz kindly helped with Alkenone analyses by MDGC. Jutta Heinze kept the clean lab running at GEOMAR and many students helped with careful sample preparation. Samples were provided by the Integrated Ocean Drilling Program (IODP). This study was supported by the "Deutsche Forschungsgemeinschaft" (DFG) and the "Deutscher Akademischer Austausch Dienst" (DAAD).

References

Andersson, C., Wanke, D.A., Channell, J.E.T., Stoner, J., Jansen, E., 2002. The Mid-Pliocene (3.6–2.6 Ma) benthic stable isotope record of the Southern Ocean: ODP Sites 1092 and 704, Meteor Rise. Palaeogeogr. Palaeoclimatol. Palaeoecol. 182, 165–181.

Arsouze, T., Dutay, J.-C., Kageyama, M., Lacan, F., Alkama, R., Marti, O., Jeandel, C., 2008. A modelling sensitivity study of the influence of the Atlantic meridional overturning circulation on neodymium isotopic composition at the Last Glacial Maximum. Clim. Past 4, 191–203.

Bartoli, G., Sarnthein, M., Weinelt, M., 2006. Late Pliocene millennial-scale climate variability in the northern North Atlantic prior to and after the onset of Northern Hemisphere glaciation. Paleoceanography 21, PA4205.

Bartoli, G., Sarnthein, M., Weinelt, M., Erlenkeuser, H., Garbe-Schönberg, D., Lea, D.W., 2005. Final closure of Panama and the onset of northern hemisphere glaciation. Earth Planet. Sci. Lett. 237, 33–44.

Bigg, G.R., Wadley, M.R., 2001. The origin and flux of icebergs into the Last Glacial Maximum Northern Hemisphere Oceans. J. Quat. Sci. 16, 565–573.

Blanc, P.L., 2002. The opening of the Plio-Quaternary Gibraltar Strait: assessing the size of a cataclysm. Geodin. Acta 15, 303–317.

Borenäs, K.M., Wåhlin, A.K., Ambar, I., Serra, N., 2002. The Mediterranean Outflow splitting: a comparison between theoretical models and CANIGO data. Deep Sea Res. 49, 4195–4205.

Bower, A.S., LeCann, B., Rossby, T., Zenk, W., Gould, J., Speer, K., Richardson, P.L., Prater, M.D., Zhang, H.M., 2002. Directly measured mid-depth circulation in the northeastern North Atlantic Ocean. Nature 419, 603–607.

Broecker, W.S., Peng, T.H., 1982. Tracers in the Sea. Lamont–Doherty Earth Observatory publication, p. 690.

Bryden, H.L., Kinder, T.H., 1991. Steady two-layer exchange through the Strait of Gibraltar. Deep-Sea Res. 38, 445–463.

Cacho, I., Grimalt, J.O., Sierro, F.J., Shackleton, N., Canals, M., 2000. Evidence for enhanced Mediterranean thermohaline circulation during rapid climatic coolings. Earth Planet. Sci. Lett. 183, 417–429.

Channell, J.E.T., Guyodo, Y., 2004. The Matuyama chronozone at ODP Site 982 (Rockall Bank): evidence for decimeter-scale magnetization lock-in depths. In: Channell, J.E. T., Kent, D.V., Lowrie, W., Meert, J. (Eds.), Timescales of the Paleomagnetic Field. Geophysical Monograph Series. 145, pp. 205–219.

Colin, C., Frank, N., Copard, K., Douville, E., 2010. Neodymium isotopic composition of deep-sea corals from the NE Atlantic: implications for past hydrological changes during the Holocene. Quat. Sci. Rev. 29, 2509–2517.

Colleoni, F., Masina, S., Negri, A., Marzocchi, A., 2012. Plio-Pleistocene high–low latitude climate interplay: a Mediterranean point of view. Earth Planet. Sci. Lett. 319–320, 35–44.

Conte, M.H., Sicre, M.-A., Rühlemann, C., Weber, J.C., Schulte, S., Schulz-Bull, D., Blanz, T., 2006. Global temperature calibration of the alkenone unsaturation index (U^{k}_{37}) in surface waters and comparison with surface sediments. Geochem. Geophys. Geosyst. 7, Q02005.

Copard, K., Colin, C., Douville, E., Freiwald, A., Gudmundson, G., De Mol, B., Frank, N., 2010. Nd isotopes in deep-sea corals in the North-eastern Atlantic. Quat. Sci. Rev. 29, 2499–2508.

Copard, K., Colin, C., Frank, N., Jeandel, C., Montero-Serrano, J.-C., Reverdin, G., Ferron, B., 2011. Nd isotopic composition of water masses and dilution of the Mediterranean outflow along the southwest European margin. Geochem. Geophys. Geosyst. 12, Q06020.

Crocket, K.C., Vance, D., Gutjahr, M., Foster, G.L., Richards, D.A., 2011. Persistent Nordic deep-water overflow to the glacial North Atlantic. Geology 39, 515–518.

Drake, N.A., El-Hawat, A.S., Turner, P., Armitage, S.J., Salem, M.J., White, K.H., McLaren, S., 2008. Palaeohydrology of the Fazzan Basin and surrounding regions: the last 7 million years. Palaeogeogr. Palaeoclimatol. Palaeoecol. 263, 131–145.

Elderfield, H., Yu, J., Anand, P., Kiefer, T., Nyland, B., 2006. Calibrations for benthic foraminiferal Mg/Ca paleothermometry and the carbonate ion hypothesis. Earth Planet. Sci. Lett. 250, 633–649.

Elmore, A.C., Piotrowski, A.M., Wright, J.D., Scrivner, A.E., 2011. Testing the extraction of past seawater Nd isotopic composition from North Atlantic deep sea sediments and foraminifera. Geochem. Geophys. Geosyst. 12, Q09008. http://dx.doi.org/10.1029/2011gc003741.

Fauquette, S., Guiot, J., Suc, J.-P., 1998. A method for climatic reconstruction of the Mediterranean Piocene using pollen data. Palaeogeogr. Palaeoclimatol. Palaeoecol. 144, 183–201.

Frajka-Williams, E., Cunningham, S.A., Kanzow, T., Johns, W.E., Meinen, C., Bryden, H.L., Baringer, M.O., McCarthy, G.D., 2012. Dramatic interannual variability in the Atlantic

Meridional Overturning Circulation (AMOC) at 26°N. Geophys. Res. Abstr. 14 (EGU2012-7661-1).
Frank, M., 2002. Radiogenic isotopes: tracers of past ocean circulation and erosional input. Rev. Geophys. 40 (1), 1001. http://dx.doi.org/10.1029/2000RG000094.
Ganssen, G., 1983. Dokumentation von küstennahem Auftrieb anhand stabiler Isotope in rezenten Foraminiferen vor Nordwest-Afrika. Meteorol. Forschungsergeb. 37, 1–46.
García-Lafuente, J., Sanchez Roman, A., Sannino, G., Sanchez Garrido, J.C., Díaz del Rio, G., 2007. Recent observations of seasonal variability of the Mediterranean outflow in the Strait of Gibraltar. J.Geophys. Res. Oceans 112, C10018.
Garrett, C., Bormans, M., Thompson, K., 1990. Is the exchange through the Straits of Gibraltar maximal or sub-maximal? In: Pratt, L.J. (Ed.), The Physical Oceanography of Sea Straits. Kluwer Academic Publisher, Boston, Mass, pp. 271–294.
Gröger, M., Henrich, R., Bickert, T., 2003. Variability of silt grain size and planktonic foraminiferal preservation in Plio/Pleistocene sediments from the western equatorial Atlantic and Caribbean. Mar. Geol. 201, 307–320.
Gutjahr, M., Frank, M., Stirling, C.H., Klemm, V., van de Flierdt, T., Halliday, A.N., 2007. Reliable extraction of a deep-water trace metal isotope signal from Fe–Mn oxyhydroxide coatings of marine sediments. Chem. Geol. 242, 351–370.
Haug, G.H., Tiedemann, R., 1998. Effect of the formation of the isthmus of Panama on Atlantic Ocean thermohaline circulation. Nature 393, 673–676.
Hecht, M., Holland, W., Artale, V., Pinardi, N., 1997. North Atlantic model sensitivity to Mediterranean waters. In: Howe, W., Henderson-Sellers, A. (Eds.), Assessing Climate Change: Results From the Model Evaluation Consortium for Climate Assessment. Gordon and Breach Science Publishers, pp. 169–191.
Holbourn, A.E., Henderson, A.S., 2002. Re-illustration and revised taxonomy for selected deep-sea benthic foraminifers. Palaeontol. Electron. 4.
Käse, R.H., Zenk, W., 1996. Structure of the Mediterranean Water and meddy characteristics in the northeastern Atlantic. In: Krauss, W. (Ed.), The Warm Water Sphere of the North Atlantic Ocean. Gebrüder Borntraeger, Berlin, Stuttgart, pp. 365–395.
Khélifi, N., Frank, M., 2014. A major change in North Atlantic deep water circulation 1.6 million years ago. Clim. Past 10, 1441–1451.
Khélifi, N., Sarnthein, M., Andersen, N., Blanz, T., Frank, M., Garbe-Schönberg, D., Haley, B.A., Stumpf, R., Weinelt, M., 2009. A major and long-term Pliocene intensification of the Mediterranean outflow, 3.5–3.3 Ma ago. Geology 37, 811–814.
Khélifi, N., Sarnthein, M., Naafs, B.D.A., 2012. Technical note: Late Pliocene age control and composite depths at ODP Site 982, revisited. Clim. Past 8, 79–87.
Kleiven, H.F., Jansen, E., Fronval, T., Smith, T.M., 2002. Intensification of Northern Hemisphere glaciations in the circum Atlantic region (3.5–2.4 Ma) — ice-rafted detritus evidence. Palaeogeogr. Palaeoclimatol. Palaeoecol. 184, 213–223.
Lacan, F., Jeandel, C., 2004. Neodymium isotopic composition and rare earth element concentrations in the deep and intermediate Nordic Seas: constraints on the Iceland Scotland Overflow Water signature. Geochem. Geophys. Geosyst. 5 Q11006.
Lacan, F., Jeandel, C., 2005. Neodymium isotopes as a new tool for quantifying exchange fluxes at the continent–ocean interface. Earth Planet. Sci. Lett. 232, 245–257.
Lawrence, K.T., Bailey, I., Raymo, M.E., 2013. Re-evaluation of the age model for North Atlantic Ocean Site 982 — arguments for a return to the original chronology. Clim. Past 9, 2391–2397. http://dx.doi.org/10.5194/cp-9-2391-2013.
Lear, C.H., Rosenthal, Y., Slowey, N., 2002. Benthic foraminiferal Mg/Ca-paleothermometry: a revised core-top calibration. Geochim. Cosmochim. Acta 66, 3375–3387.
Lisiecki, L.E., Raymo, M.E., 2005. A Pliocene–Pleistocene stack of 57 globally distributed benthic $\delta^{18}O$ records. Paleoceanography 20, PA1003.
Louarn, E., Morin, P., 2011. Antarctic intermediate water influence on Mediterranean Sea water outflow. Deep Sea Res. I 58, 932–942.
Loubere, P., 1987a. Late Pliocene variations in the carbon isotope values of North Atlantic benthic foraminifera: biotic control of the isotopic record? Mar. Geol. 76, 45–56.
Loubere, P., 1987b. Changes in mid-depth North Atlantic and Mediterranean circulation during the Late Pliocene — isotopic and sedimentological evidence. Mar. Geol. 77, 15–38.
Loubere, P., 1988. Gradual late Pliocene onset of glaciation: a deep-sea record from the Northeast Atlantic. Palaeogeogr. Palaeoclimatol. Palaeoecol. 63, 327–334.
Lozier, M.S., Stewart, N.M., 2008. On the temporally varying northward penetration of Mediterranean outflow water and eastward penetration of Labrador Sea Water. J. Phys. Oceanogr. 38, 2097–2103.
McCartney, M.S., Mauritzen, C., 2001. On the origin of the warm inflow to the Nordic Seas. Prog. Oceanogr. 51, 125–214.
Miller, K.G., Wright, J.D., Browning, J.V., Kulpecz, A., Kominz, M., Naish, T.R., Cramer, B.S., Rosenthal, Y., Peltier, W.R., Sosdian, S., 2012. High tide of the warm Pliocene: implications of global sea level for Antarctic deglaciation. Geology 40, 407–410.
Millot, C., 1999. Circulation in the western Mediterranean Sea. J. Mar. Syst. 20, 423–442.
Montero-Serrano, J.C., Frank, N., Colin, C., Wienberg, C., Eisele, M., 2011. The climate influence on the mid-depth Northeast Atlantic gyres viewed by cold-water corals. Geophys. Res. Lett. 38, L19604. http://dx.doi.org/10.1029/2011GL048733.
Muiños, S.B., Frank, M., Maden, C., Hein, J.R., van de Flierdt, T., Lebreiro, S.M., Gaspar, L., Monteiro, J.H., Halliday, A.N., 2008. New constraints on the Pb and Nd isotopic evolution of NE Atlantic water masses. Geochem. Geophys. Geosyst. 9, Q02007.
New, A.L., Barnard, S., Herrmann, P., Molines, J.-M., 2001. On the origin and pathway of the saline inflow to the Nordic Seas: insights from models. Prog. Oceanogr. 48, 255–287.
NODC, 2001. National Oceanographic and Data Center, World Ocean Atlas 2001, objective analyses, data statistics, and figures. CD-ROM documentation. http://www.nodc.noaa.gov/.
O'Neill-Baringer, M., Price, J.F., 1997. Mixing and spreading of the Mediterranean outflow. J. Phys. Oceanogr. 27, 1654–1677.
O'Neill-Baringer, M., Price, J.F., 1999. A review of the physical oceanography of the Mediterranean outflow. Mar. Geol. 155, 63–82.
O'Nions, R.K., Frank, M., von Blanckenburg, F., Ling, H.-F., 1998. Secular variation of Nd and Pb isotopes in ferromanganese crusts from the Atlantic, Indian and Pacific Oceans. Earth Planet. Sci. Lett. 155, 15–28.
Ostermann, D.R., Curry, W.B., 2000. Calibration of stable isotopic data: an enriched $\delta^{18}O$ standard used for source gas mixing detection and correction. Paleoceanography 15, 353–360.
Pierre, C., 1999. The oxygen and carbon isotope distribution in the Mediterranean water masses. Mar. Geol. 153, 41–55.
Prahl, F.G., Wakeham, S.G., 1987. Calibration of unsaturation patterns in long-chain ketone compositions for paleotemperature assessment. Nature 330, 367–369.
Price, J.F., Yang, J.Y., 1998. Marginal sea overflows for climate simulations. In: Chassignet, E.P., Verron, J. (Eds.), Ocean Modeling and Parameterization. Springer, Dordrecht, Netherlands, pp. 155–170.
Rahmstorf, S., 1998. Influence of Mediterranean outflow on climate. Eos, Trans. Am. Geophys. Union 79, 281.
Ravelo, A.C., Andreasen, D.H., 2000. Enhanced circulation during a warm period. Geophys. Res. Lett. 27, 1001–1004.
Raymo, M.E., Mitrovica, J.X., O'Leary, M.J., DeConto, R.M., Hearty, P.J., 2011. Departures from eustasy in Pliocene sea-level records. Nat. Geosci. 4, 328–332.
Reid, J.L., 1979. On the contribution of the Mediterranean Sea outflow to the Norwegian–Greenland Sea. Deep-Sea Res. I 26, 1199–1223.
Rempfer, J., Stocker, T.F., Joos, F., Dutay, J.-C., Siddall, M., 2011. Modelling Nd-isotopes with a coarse resolution ocean circulation model: sensitivities to model parameters and source/sink distributions. Geochim. Cosmochim. Acta 75, 5927–5950.
Rickli, J., Frank, M., Halliday, A.N., 2009. The hafnium–neodymium isotopic composition of Atlantic seawater. Earth Planet. Sci. Lett. 280, 118–127.
Robinson, L.F., Adkins, J.F., Frank, N., Gagnon, A.C., Prouty, N.G., Brendan Roark, E., van de Flierdt, T., 2014. The geochemistry of deep-sea coral skeletons: a review of vital effects and applications for palaeoceanography. Deep-Sea Res. II Top. Stud. Oceanogr. 99, 184–198.
Rogerson, M., Rohling, E.J., Bigg, G.R., Ramirez, J., 2012. Paleoceanography of the Atlantic–Mediterranean exchange: overview and first quantitative assessment of climatic forcing. Rev. Geophys. 50, RG2003.
Sarnthein, M., Bartoli, G., Prange, M., Schmittner, A., Schneider, B., Weinelt, M., Andersen, N., Garbe-Schönberg, D., 2009. Mid-Pliocene shifts in ocean overturning circulation and the onset of Quaternary-style climates. Clim. Past 5, 269–283.
Sarnthein, M., Winn, K., Jung, S.J.A., Duplessy, J.-C., Labeyrie, L., Erlenkeuser, H., Ganssen, G., 1994. Changes in east Atlantic deepwater circulation over the last 30,000 years: eight time slice reconstructions. Paleoceanography 9, 209–267.
Schlitzer, R., 2013. Ocean data view. (available at) http://odv.awi.de.
Serrano, F., González-Donoso, J.M., Palmqvist, P., Guerra-Merchán, A., Linares, D., Pérez-Claros, J.A., 2007. Estimating Pliocene sea-surface temperatures in the Mediterranean: An approach based on the modern analogs technique. Palaeogeogr. Palaeoclimatol. Palaeoecol. 243, 174–188.
Shackleton, N.J., 1974. Attainment of isotopic equilibrium between ocean water and the benthonic foraminifera genus *Uvigerina*: isotopic changes in the ocean during the last glacial. Colloq. Int. du Cent. Natl du Rech. Sci. 219, 203–210.
Shipboard Scientific Party, 1985. Proceedings of the Deep Sea Drilling Project — Initial Reports, 80. U.S. Govt. (Site 548) In: Graciansky, P.C., de Poag, C.W. (Eds.), Printing Office, Washington, pp. 33–122.
Shipboard Scientific Party, 1996. Proceedings of the Ocean Drilling Program — Initial Reports, 161. In: Comas, M.C., Zahn, R., Klaus, A. (Eds.), College Station, TX (Ocean Drilling Program), pp. 355–388.
Sosdian, S., Rosenthal, Y., 2009. Deep-sea temperature and ice volume changes across the Pliocene–Pleistocene climate transitions. Science 325, 306–310.
Spivack, A.J., Wasserburg, G.J., 1988. Neodymium isotopic composition of the Mediterranean outflow and the eastern North Atlantic. Geochim. Cosmochim. Acta 58, 2767–2773.
Stumpf, R., Frank, M., Schönfeld, J., Haley, B.A., 2010. Late Quaternary variability of Mediterranean Outflow Water from radiogenic Nd and Pb isotopes. Quat. Sci. Rev. 29, 2462–2472.
Tachikawa, K., Roy-Barman, M., Michard, A., Thouron, D., Yeghicheyan, D., Jeandel, C., 2004. Neodymium isotopes in the Mediterranean Sea: comparison between seawater and sediment signals. Geochim. Cosmochim. Acta 68, 3095–3106.
Tsimplis, M.N., Bryden, H.L., 2000. Estimation of the transports through the strait of Gibraltar. Deep Sea Res. 47, 2219–2242.
van Morkhoven, F.P.C.M., Berggren, W.A., Edwards, A.S., 1986. Cenozoic cosmopolitan deep-water benthic foraminifera. Bulletin des Centres de Recherches Exploration–Production. Elf-Aquitaine Memoir 11, 406.
Venz, K.A., Hodell, D.A., 2002. New evidence for changes in Plio-Pleistocene deep water circulation from Southern Ocean ODP Leg 177 Site 1090. Palaeogeogr. Palaeoclimatol. Palaeoecol. 182, 197–220.
Voelker, A.H.L., Lebreiro, S.M., Schönfeld, J., Cacho, I., Erlenkeuser, H., Abrantes, F., 2006. Mediterranean outflow strengthening during Northern Hemisphere coolings: a salt source for the glacial Atlantic? Earth Planet. Sci. Lett. 245, 39–55.
von Blanckenburg, F., 1999. Tracing past ocean circulation? Science 286, 1862–1863.
Wu, W., Danabasoglu, G., Large, W.G., 2007. On the effects of parameterized Mediterranean overflow on North Atlantic ocean circulation and climate. Ocean Model. 19, 31–52.
Yu, J.M., Elderfield, H., 2008. Mg/Ca in the benthic foraminifera *Cibicidoides wuellerstorfi* and *Cibicidoides mundulus*: temperature versus carbonate ion saturation. Earth Planet. Sci. Lett. 276, 129–139.
Zahn, R., Sarnthein, M., Erlenkeuser, H., 1987. Benthic isotope evidence for changes of the Mediterranean outflow during the Late Quaternary. Paleoceanography 2, 543–559.
Zahn, R., Schönfeld, J., Kudrass, H.-R., Park, M.-H., Erlenkeuser, H., Grootes, P., 1997. Thermohaline instability in the North Atlantic during meltwater events: stable isotope and ice-rafted detritus records from Core SO75-26KL, Portuguese Margin. Paleoceanography 12, 696–710.
Zenk, W., Armi, L., 1990. The complex spreading pattern of Mediterranean water off the Portuguese continental slope. Deep-Sea Res. I 37, 1805–1823.

Further Reading

Becker, J., Lourens, L.J., Raymo, M.E., 2006. High-frequency climate linkages between the North Atlantic and the Mediterranean during marine oxygen isotope stage 100 (MIS100). Paleoceanography 21, PA3002.

Bemis, B.E., Spero, H.J., Bijma, J., Lea, D.W., 1998. Reevaluation of the oxygen isotopic composition of planktonic foraminifera: experimental results and revised paleotemperature equations. Paleoceanography 13, 150–160.

Béthoux, J.-P., Pierre, C., 1999. Mediterranean functioning and sapropel formation: respective influences of climate and hydrological changes in the Atlantic and the Mediterranean. Mar. Geol. 153, 29–39.

Billups, K., Ravelo, A.C., Zachos, J.C., 1998. Early Pliocene deep water circulation in the western equatorial Atlantic: implications for high-latitude climate change. Paleoceanography 13, 84–95.

Cacho, I., Shackleton, N., Elderfield, H., Sierro, F.J., Grimalt, J.O., 2006. Glacial rapid variability in deep-water temperature and $\delta^{18}O$ from the Western Mediterranean Sea. Quat. Sci. Rev. 25, 3294–3311.

Cane, M., Molnar, P., 2001. Closing of the Indonesian seaway as a precursor to east African aridification around 3–4 million years ago. Nature 411, 157–162.

Cerling, T.E., Wynn, J.G., Andanje, S.A., Bird, M.I., Korir, D.K., Levin, N.E., Mace, W., Macharia, A.N., Quade, J., Remien, C.H., 2011. Woody cover and hominin environments in the past 6 million years. Nature 476 (7358), 51–56.

Channell, J.E.T., Lehman, B., 1999. Magnetic stratigraphy of North Atlantic Sites 980–984. In: Raymo, M.E., Jansen, E., Blum, P., Herbert, T.D. (Eds.), Proceedings of the Ocean Drilling Program — Scientific Results, 162. College Station. TX (Ocean Drilling Program), pp. 113–130.

Cita, M.B., 1973. Mediterranean evaporite: paleontological arguments for a deep basin desiccation model. In: Drooger, C.W. (Ed.), Messinian Events in the Mediterranean. Elsevier, Amsterdam, pp. 206–228.

Cohen, A.S., O'Nions, R.K., Siegenthaler, R., Griffin, W.L., 1988. Chronology of the pressure–temperature history recorded by a granulite terrain. Contrib. Mineral. Petrol. 98, 303–311.

Combourieu-Nebout, N., 1991. Late Pliocene Northern Hemisphere glaciations: the continental and marine responses in the central Mediterranean. Quat. Sci. Rev. 10, 319–334.

Craig, H., Gordon, L.I., 1965. Deuterium and oxygen 18 variations in the ocean and the marine atmosphere. In: Tongiorgi, E. (Ed.), Proceedings of a Conference on Stable Isotopes in Oceanographic Studies and Paleotemperatures, Spoleto. Italy. V. Lishi e F, Pisa, pp. 9–130.

Curry, W.B., Oppo, D.W., 2005. Glacial water mass geometry and the distribution of $\delta^{13}C$ of $\sum CO_2$ in the western Atlantic Ocean. Paleoceanography 20, PA1017.

de Villiers, S., Greaves, M., Elderfield, H., 2002. An intensity ratio calibration method for the accurate determination of Mg/Ca and Sr/Ca of marine carbonates by ICP-AES. Geochem. Geophys. Geosyst. 3, 1001.

deMenocal, P.B., 1995. Plio-Pleistocene African climate. Science 270, 53–59.

Driscoll, N.W., Haug, G., 1998. A short circuit in thermohaline circulation: a cause for Northern Hemisphere glaciation. Science 282, 436–438.

Frank, M., Whiteley, N., Kasten, S., Hein, J.R., O'Nions, K., 2002. North Atlantic deep water export to the Southern Ocean over the past 14 Myr: evidence from Nd and Pb isotopes in ferromanganese crusts. Paleoceanography 17, 1022.

Ganachaud, A., Wunsch, C., 2000. Improved estimates of global ocean circulation, heat transport and mixing from hydrographic data. Nature 408, 453–457.

Garzoli, S., Maillard, C., 1979. Winter circulation in the Sicily and Sardinia straits region. Deep-Sea Res. 26A, 933–954.

Hayashi, T., Ohno, M., Acton, G., Guyodo, Y., Evans, H.F., Kanamatsu, T., Komatsu, F., Murakami, F., 2010. Millennial scale iceberg surges after intensification of Northern Hemisphere glaciation. Geochem. Geophys. Geosyst. 11, Q09Z20.

Jacobsen, S.B., Wasserburg, G.J., 1980. Sm–Nd isotopic evolution of chondrites. Earth Planet. Sci. Lett. 50, 139–155.

Karas, C., Nürnberg, D., Gupta, A., Tiedemann, R., Mohan, K., Bickert, T., 2009. Mid-Pliocene climate change amplified by a switch in Indonesian subsurface throughflow. Nat. Geosci. 2, 433–437.

Käse, R.H., Zenk, W., 1987. Reconstructed Mediterranean salt lens trajectories. J. Phys. Oceanogr. 17, 158–163.

Keigwin, L.D., 1987. Pliocene stable-isotope record of Deep Sea Drilling Project Site 606: sequential events of ^{18}O enrichment beginning at 3.1 Ma. In: Ruddiman, W.F., et al. (Eds.), Proceedings of the Deep Sea Drilling Project — Initial Reports. 94, pp. 911–920.

Krijgsman, W., Hilgen, F.J., Raffi, I., Sierro, F.J., Wilson, D.S., 1999. Chronology, causes and progression of the Messinian salinity crisis. Nature 400, 652–655.

Lawrence, K.T., Herbert, T.D., Brown, C.M., Raymo, M.E., Haywood, A.M., 2009. High-amplitude variations in North Atlantic sea surface temperature during the early Pliocene warm period. Paleoceanography 24, PA2218.

Levin, N., Quade, J., Simpson, S.W., Semaw, S., Rogers, M., 2004. Isotopic evidence for Plio-Pleistocene environmental change at Gona, Ethiopia. Earth Planet. Sci. Lett. 219, 93–110.

Llave, E., Matias, H., Hernández-Molina, F.J., Ercilla, G., Stow, D.A.V., Medialdea, T., 2011. Pliocene–Quaternary contourites along the northern Gulf of Cadiz margin: sedimentary stacking pattern and regional distribution. Geo-Mar. Lett. 31, 377–390.

Lourens, L.J., Hilgen, F.J., Gudjonsson, L., Zachariasse, W.J., 1992. Late Pliocene to early Pleistocene astronomically forced sea surface productivity and temperature variations in the Mediterranean. Mar. Micropaleontol. 19, 49–78.

Lunt, D.J., Valdes, P.J., Haywood, A., Rutt, I.C., 2007. Closure of the Panama Seaway during the Pliocene: implications for climate and Northern Hemisphere glaciation. Clim. Dyn. 30, 1–18.

Martin, P.A., Lea, D.W., 2002. A simple evaluation of cleaning procedures on fossil benthic foraminiferal Mg/Ca. Geochem. Geophys. Geosyst. 3, 8401.

Martrat, M., Grimalt, J.O., López-Martínez, C., Cacho, I., Sierro, F.J., Flores, J.A., Zahn, R., Canals, M., Curtis, J.H., Hodell, D.A., 2004. Abrupt temperature changes in the western Mediterranean during the last and penultimate glacial and interglacial periods. Science 306, 1762–1765.

Maslin, M.A., Trauth, M.H., 2009. Plio-Pleistocene East African pulsed climate variability and its influence on early human evolution. In: Grine, F.E., Leakey, R.E., Fleagle, J.G. (Eds.), The First Humans — Origins of the Genus *Homo*Vertebrate Paleobiology and Paleoanthropology Series. Springer Verlag, pp. 151–158.

McManus, J.F., Francois, R., Gherardi, J.-M., Keigwin, L.D., Brown-Ledger, S., 2004. Collapse and rapid resumption of Atlantic meridional circulation linked to deglacial climate changes. Nature 428, 834–837.

Molnar, P., England, P., Martinod, J., 1993. Mantle dynamics, uplift of the Tibetan Plateau, and the Indian Monsoon. Rev. Geophys. 31, 357–396.

Naafs, B.D.A., Stein, R., Hefter, J., Khélifi, N., De Schepper, S., Haug, G.H., 2010. Late Pliocene changes in the North Atlantic current. Earth Planet. Sci. Lett. 298, 434–442.

Pachur, H.J., Altmann, N., 2006. Die Ostsahara im Spätquartär. Springer, Berlin, New York, p. 662.

Paillard, D., Labeyrie, L., Yiou, P., 1996. Macintosh program performs time-series analysis. Eos, Trans. Am. Geophys. Union 77, 379.

Paterne, M., Kallel, N., Labeyrie, L., Vautravers, M., Duplessy, J.-C., Rossignol-Strick, M., Cortijo, E., Arnold, M., Fontugne, M., 1999. Hydrological relationship between the North Atlantic Ocean and the Mediterranean Sea during the past 15–75 kyr. Paleoceanography 14, 626–638.

Piotrowski, A.M., Goldstein, S.L., Hemming, S.R., Fairbanks, R.G., 2005. Temporal relationships of carbon cycling and ocean circulation at glacial boundaries. Science 307, 1933–1938.

Rodgers, K.B., Latif, M., Legutke, S., 2000. Sensitivity of equatorial Pacific and Indian Ocean watermasses to the position of the Indonesian throughflow. Geophys. Res. Lett. 27, 2941–2944.

Rohling, E.J., 2000. Paleosalinity: confidence limits and future applications. Mar. Geol. 163, 1–11.

Rohling, E.J., Abu-Zied, R., Casford, J.S.L., Hayes, A., Hoogakker, B.A.A., 2009. The marine environment: present and past. In: Woodward, J.C. (Ed.), The Physical Geography of the Mediterranean. Oxford University Press, pp. 33–67.

Rohling, E.J., Cane, T.R., Cooke, S., Sprovieri, M., Bouloubassi, I., Emeis, K.C., Schiebel, R., Kroon, D., Jorissen, F.J., Lorre, A., Kemp, A.E.S., 2002. African monsoon variability during the previous interglacial maximum. Earth Planet. Sci. Lett. 202, 61–75.

Rohling, E.J., Hayes, A., De Rijk, S., Kroon, D., Zachariasse, W.J., Eisma, D., 1998. Abrupt cold spells in the northwest Mediterranean. Paleoceanography 13, 316–322.

Roque, C., Duarte, H., Terrinha, P., Valadares, V., Noiva, J., Cachão, M., Ferreira, J., Legoinha, P., Zitellini, N., 2012. Pliocene and Quaternary depositional model of the Algarve margin contourite drifts (Gulf of Cadiz, SW Iberia): seismic architecture, tectonic control and paleoceanographic insights. Mar. Geol. 303–306, 42–62.

Spaak, P., 1983. Accuracy in correlation and ecological aspects of the planktonic foraminiferal zonation of the Mediterranean Pliocene. Utrecht Micropaleontol. Bull. 28, 168.

Rossignol-Strick, M., 1985. Mediterranean Quaternary sapropels, an immediate response of the African monsoon to variation of insolation. Palaeogeogr. Palaeoclimatol. Palaeoecol. 49, 237–263.

Suc, J.P., 1984. Origin and evolution of the Mediterranean vegetation and climate in Europe. Nature 307, 429–432.

Tanaka, T., Togashi, S., Kamioka, H., et al., 2000. JNdi-1: a neodymium isotopic reference in consistency with LaJolla neodymium. Chem. Geol. 168, 279–281.

Thunell, R.C., Williams, D.F., Howell, M., 1987. Atlantic–Mediterranean water exchange during the late Neogene. Paleoceanography 2, 661–678.

Thunell, R.T., Williams, D., Tappa, E., et al., 1990. Plio-Pleistocene stable isotope record for ocean drilling program Site 653, Tyrrhenian Basin: implications for the paleoenvironmental history of the Mediterranean Sea. Proceedings of the Ocean Drilling Program — Scientific Results. 107, pp. 387–399.

Tiedemann, R., Sarnthein, M., Shackleton, N.J., 1994. Astronomic timescale for the Pliocene Atlantic $\delta^{18}O$ and dust flux records of Ocean Drilling Program Site 659. Paleoceanography 9, 619–638.

Townsend, H.A., 1985. The paleomagnetism of sediments acquired from the Goban Spur on DSDP Leg 80. Proceedings of the Deep Sea Drilling Project — Initial Reports, 80U. S. Govt. Printing Office, Washington, pp. 389–414.

Trauth, M.H., Maslin, M.A., Deino, A., et al., 2005. Late Cenozoic moisture history of East Africa. Science 309, 2051–2053.

Tzedakis, P.C., 2007. Seven ambiguities in the Mediterranean palaeoenvironmental narrative. Quat. Sci. Rev. 26, 2042–2066.

Vergnaud-Grazzini, C., Saliège, J.-F., Urrutiaguer, M.-J., et al., 1990. Oxygen and Carbon Isotope Stratigraphy of ODP Hole 653A and Site 654: The Pliocene–Pleistocene Glacial History Recorded in the Tyrrhenian Basin (West Mediterranean), ODP Leg 107B. 107. Proceedings of the Ocean Drilling Program — Scientific Results, pp. 361–386.

Willis, K.J., Kleckowski, A., Crowhurst, S.J., 1999. 124,000-year periodicity in terrestrial vegetation change during the late Pliocene epoch. Nature 397, 685–688.

Wüst, G., 1961. On the vertical circulation of the Mediterranean Sea. J. Geophys. Res. 66, 3261–3271.

Zachariasse, W.J., Gudjonsson, L., Hilgen, F.J., Langereis, C.G., Lourens, L.J., Verhallen, P.J.J.M., Zijderveld, J.D.A., 1990. Late Gauss to Early Matuyama invasions of *Neogloboquadrina Atlantica* in the Mediterranean and associated record of climatic change. Paleoceanography 5, 239–252.